Miner Petrol (2012) 106:217–242
DOI 10.1007/s00710-012-0227-5

ORIGINAL PAPER

Mineralogy, geochemistry and petrogenesis of the recent magmatic formations from Mbengwi, a continental sector of the Cameroon Volcanic Line (CVL), Central Africa

Benoît Joseph Mbassa · Emmanuel Njonfang · Mathieu Benoit · Pierre Kamgang · Michel Grégoire · Stephanie Duchene · Pierre Brunet · Bekoa Ateba · Félix M. Tchoua

Received: 2 February 2012 / Accepted: 5 October 2012 / Published online: 25 October 2012

Abstract The Mbengwi recent magmatic formations consist of volcanics and syenites belonging to the same magmatic episode. Lavas form a bimodal basanite-rhyolite alkaline series with a gap between 50 and 62 wt.% SiO_2. Mafic lavas (basanite-hawaiite) are sodic while felsic rocks (trachyte-rhyolite-syenites) are sodi-potassic, slightly metaluminous to peralkaline. The geochemical and isotopic characteristics ($0.7031<(^{87}Sr/^{86}Sr)_{initial}<0.7043$; $1.03<\varepsilon_{Ndi}<5.17$) of these rocks are similar to those of other rocks from the CVL. The main differentiation process is fractional crystallization with two trends of fractionation. Their Rb/Sr isochron age of 28.2 Ma, almost similar to 27.40±0.6 MaK/Ar age obtained in a trachyte from neighboring Bamenda Mountains system, precludes any local age migration of an hypothetic hotspot. Mafic lavas have OIB features displaying an isotopic signature similar to that of HIMU mantle source different from FOZO known as source of most parental magmas along the CVL.

Editorial handling: B. De Vivo

B. J. Mbassa · B. Ateba
Institut de Recherches Géologiques et Minières,
IRGM/ARGV Ekona,
B.P. 370, Buéa, Cameroon

E. Njonfang
Laboratoire de Géologie, Ecole Normale Supérieure,
Université de Yaoundé I,
B.P. 47 Yaoundé, Cameroon

M. Benoit · M. Grégoire (✉) · S. Duchene · P. Brunet
Géosciences-Environnement-Toulouse Unité Mixte de Recherche
5563, Observatoire Midi Pyrénées, Université Paul Sabatier,
14, avenue Édouard-Belin,
31400 Toulouse, France
e-mail: michel.gregoire@get.obs-mip.fr

B. J. Mbassa · P. Kamgang · F. M. Tchoua
Département des Sciences de la Terre, Faculté des Sciences,
Université de Yaoundé I,
B.P. 812, Yaoundé, Cameroon

Introduction

The Cameroon volcanic line (CVL) is a tectono-magmatic structure characterized by an alignment of oceanic and continental volcanoes extending on more than 1,600 km. The line strikes almost SW-NE forming a swell and basin structure, the six oceanic islands and four continental central volcanoes representing swell (Burke, 2001) (Fig. 1b). The central volcanoes include the still active Mount Cameroon, the Manengouba, Bambouto-Bamenda and Oku Mountains. Few of these massifs have been studied. The available petrological and geochemical data show that rocks generally range from basalts, basanites, and hawaiites to trachytes, rhyolites and/or phonolites in a given massif defining a bimodal series, except at the continent-ocean boundary where Bioko and Mount Cameroon are mainly basaltic. However a few massifs including Manengouba Mountains (Kagou Dongmo et al. 2001) and the Bamenda-Bambouto display a complete range from basic to felsic rocks, characterized by a great abundance of mafic and felsic lavas and relatively rare occurrence of intermediate terms (mugearites and benmoreites) (Marzoli et al. 1999, 2000; Kamgang et al. 2007, 2008). Geochronological data reveal that the oldest volcanic ages (K-Ar) so far obtained (51.8±1.2 Ma and 46.7±1.1 Ma) are respectively in the

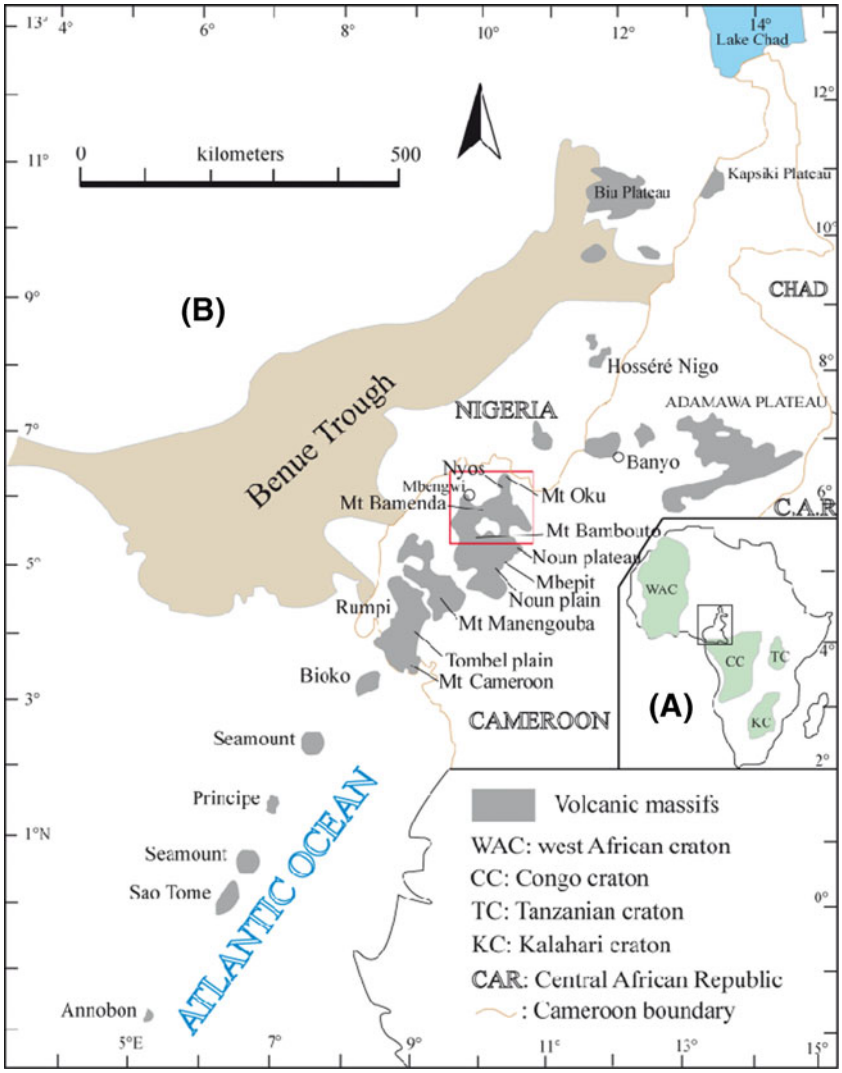

Fig. 1 The study area: **a**) Location of Cameroon in Africa; CC=Congo craton, KC=Kalahari craton, WAC=West African craton, TC=Tanzanian craton. **b**) Location of the Western Cameroon highland (*red square*) along the CVL. **c** Location of the study area (*white square*) within the Western Cameroon highland

transitional lavas and in an olivine basalt from the Bamoun Plateau (Moundi et al. 2007). According to these data, the magmatic activity along the CVL can be divided into three periods: i) the first (73–40 Ma) which is well expressed on the anorogenic complexes and of the Bamoun plateau; ii) the second (40 Ma–30 Ma), represented by the volcanoes of the northern Cameroon (Benue trough, Kapsiki plateau, and Golda Zuelva), and iii) the last (Upper Eocene to Recent) characterized by the appearance of magmatism in the oceanic sector with an episodical synchronous volcanicity. A local SW younging age has been suggested in the West Cameroon highlands from Mount Oku (31 Ma) to Bambouto (14 Ma) (Marzoli et al. 2000). Kagou Dongmo et al. (2010) has even obtained in the Bambouto Mountains a younger age of 0.48±0.01 Ma (K-Ar) in basalts. The K-Ar age range (27.40–12.7 Ma) recently obtained in the felsic lavas of Bamenda mountains (Kamgang et al. 2010) seem not to be in accordance with this hypothesis.

In order to contribute to this debate, the detail study of recent magmatic rocks of Mbengwi area, located NW to the Bamenda Mountains, has been undertaken. This study led us to the discovery of a syenitic intrusion associated with the lavas, both representing the last magmatic event having affected the Mbengwi Pan-African granitoids. Their petrological and geochemical and isotopic data are presented in this paper. The aim is to constrain their petrogenesis and to compare the results with those of the neighboring Bamenda Mountains in particular and the whole CVL in general.

Regional geological setting

The Mbengwi area geographically bounded by the latitudes 6°06′ and 5°58′North and the longitudes 9°57′ and 10°06′East (Fig. 1c) is located within the Western Cameroon highlands (Bambouto, Bamenda and Oku Mountains).

The neighboring Bamenda Mountains situated between 5°40′N and 6°10′N and 10°00′E and 10°30′E is the fourth

Fig. 1 (continued)

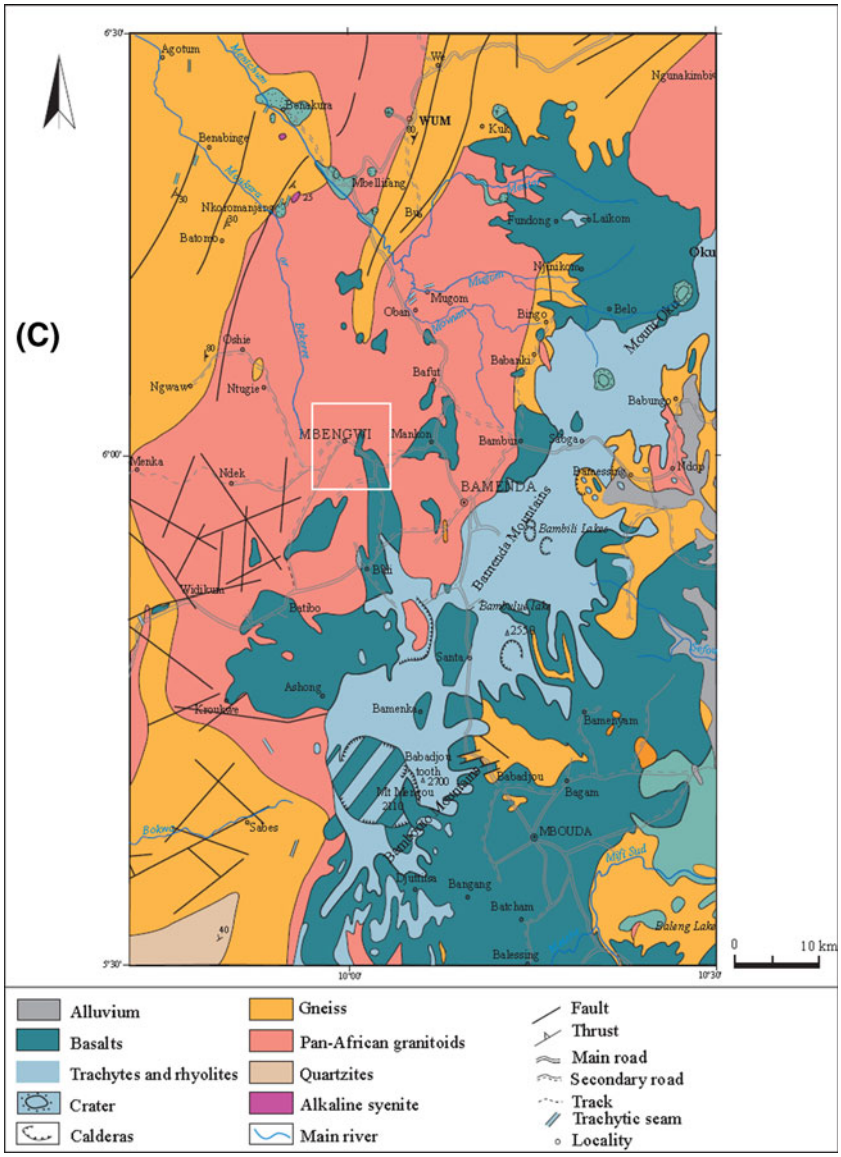

more important volcano (in volume) of the CVL. It appears as the NE prolongation of Mounts Bambouto with which there is no clear limit. The massif culminates at 2,621 m (Bambili Lake borders) and lay on a Pan-African granitic basement (Toteu et al. 2001; Nzolang et al. 2003). Mafic lavas include basanites, basalts, and hawaiites whereas intermediate and felsic lavas comprise few benmoreites and mugearites and abundant trachytes, rhyolites and pyroclastic flow deposits (Gountié Dedzo et al. 2011). Mafic and intermediate rocks are alkaline and felsic ones are mainly metaluminous to peralkaline. K-Ar dating (Kamgang et al. 2010) shows that felsic lavas are older than mafic lavas (27.40–18.98 Ma and 17.4 Ma to the present).

The Bambouto Mountains and Oku massif volcanoes are also dominated by felsic lavas relative to mafic ones. Like in the Bamenda Mountains, felsic lavas are older (Marzoli et al. 1999, 2000) and include abundant trachytes, less abundant rhyolites and subordinate benmoreites whereas mafic lavas are made up of basanites and basalts with minor hawaiites and mugearites. Mafic lavas are generally alkaline and felsic rocks alkaline to peralkaline; but a few lavas with transitional affinities have been published (Marzoli et al. 2000). As in the other massifs of the CVL, fractional crystallization sometimes associated with crustal contamination of a mantle derived melt is the main differentiation process of the Western Cameroon highlands (Marzoli et al. 1999, 2000; Kamgang et al. 2010).

The Mbengwi area is marked by the abundance of Pan-African basement rocks relative to Tertiary magmatic rocks. The Pan-African basement rocks consist mainly of heterogeneous and syntectonic granitoids enclosing locally xenoliths of gneisses and/or amphibolites. The basement in which the recent magmatic rocks here

studied are emplaced includes monzogabbro, monzonite, granodiorite, granite.

Analytical methods

Eighteen representative samples of both plutonic and volcanic rocks have been analyzed at the Ecole des Mines of Saint Etienne (France) for major elements, at ALS Minerals laboratory of Sevilla (Spain) for trace elements in felsic rocks and at the department Geosciences Environment Toulouse (GET-OMP-University of Toulouse 3, France) for trace elements (lavas) and for Nd and Sr isotopes. Major elements and trace elements analyses have been made by ICP-OES (Inductively Coupled Plasma—Optical Emission Spectrometry) and ICP-MS (Mass Spectrometry) methods respectively. International geostandards have been used and details of the methods are available in Weis and Frey (1991), Benoit et al. (1996), Aries et al. (2000), Ore Research and Exploration (2004). The Standard deviation for trace elements analysis was typically below 2 wt.%, 0.92 wt.% for SiO_2, 326.6 ppm for TiO_2, 0.45 wt.% for Al_2O_3, 0.09 wt.% for Fe_2O_3, 75.55 ppm for MnO, 0.14 wt.% for MgO, 0.26 wt.% for CaO, 0.19 wt.% for Na_2O, 753.10 ppm for K_2O and 249.50 ppm for P_2O_5. The detection limits for trace elements range from 0.01 ppm (REE) to 20 ppm (Zr). Mineral compositions have been analyzed with a CAMECA SX 50, at the service of microanalysis and microscopy of the GET. The analytical conditions were 15 kV for the acceleration tension and the beam size was 2×2 μm under 10 or 20 ηA, according to resistance of mineral to the electronic beam. Acquisition times were 10s for the peak, and 5 s on both sides of the peak, for an analyzed volume of 5 μm^3. Kα lines were used.

Isotopic measurements of Sr and Nd were eluted after HF/HNO_3 digestion using Eichrom Sr-Spec, Thru-Spec and Ln-Spec resins. The measurements were performed on a Finnigan 261 multicollector thermal-ionization mass spectrometer. Sr isotopic ratios are corrected for mass fractionation with normalization to $^{86}Sr/^{88}Sr=0.1194$. Replicate analyses of the NBS 987 standard yielded an average $^{87}Sr/^{86}Sr$ value of 0.710255±0.00002. Nd isotopic data are corrected for mass fractionation by normalization to ratio $^{146}Nd/^{144}Nd=0.7219$. Replicate analyses of the La Jolla Nd standard yielded an average $^{143}Nd/^{144}Nd$ value of 0.511850±0.00001.

Nomenclature and petrography

The late magmatic rocks of Mbengwi consist of mafic and felsic rocks. In the (Na_2O+K_2O) vs SiO_2 wt.% diagram of Le Bas et al. (1986) (Fig. 2), mafic lavas fall in the field of basanite, basalt, hawaiite and mugearite, while felsic rocks correspond to trachytes, rhyolites and syenites. Some samples of basanite (E30) and hawaiites (E7-1) display centimetric serpentinized mantle xenocrysts of olivine (Fo_{87-89}) probably resulting from the disaggregation of peridotite, but their modal amount is not enough to affect significantly the whole rock chemistry. In general, mafic lavas have microlitic aphyric or porphyritic textures (Fig. 3). Plagioclase, olivine, pyroxene and opaque minerals are the main phenocrysts phases. The groundmass is cryptocrystalline and consists of olivine microcrystals; plagioclase microlites showing in some samples a preferential orientation, opaque minerals, and accessory apatite. Secondary minerals include carbonates.

Trachytes are dark green, sometimes brecciated with fragments of trachytic lavas and of granitic basement. They are porphyritic and their groundmass consists mainly of finely crystallized alkali feldspar (≈ 60 %), clinopyroxene (≈10 %) and opaque minerals (≈15 %). The phenocrysts are mainly alkali feldspar (8–10 %), clinopyroxene (1–3 %), opaque minerals (5–7 %) and most of them except the opaque minerals are crowned. Opaque mineral microcrystals are rounded or angular, and are included in clinopyroxene crystals, or associated with carbonates around which they form a crown, while phenocrysts, up to 1 mm long, are generally corroded or reabsorbed by the groundmass and include plagioclase, olivine or zircon in some samples.

Rhyolites are ashy to greenish grey. Quartz (1 mm) and alkali feldspar phenocrysts sometimes form aggregates.

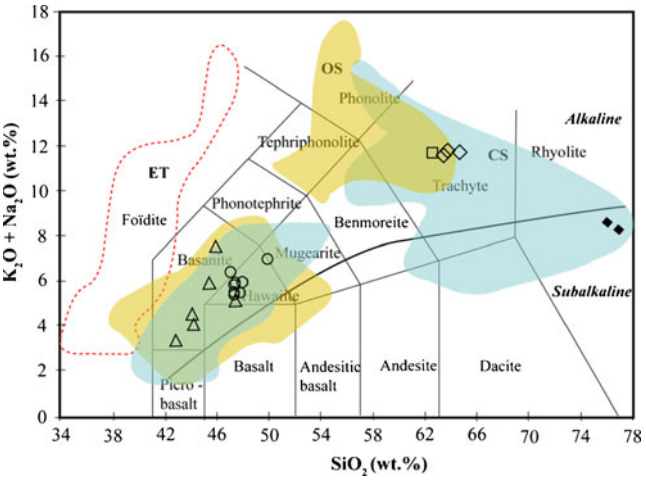

Fig. 2 Total alkali–silica (wt.%) diagram according to Le Bas et al. (1986). The Mbengwi recent formations fall mainly in basanites, hawaiites, mugearites, trachytes and rhyolites fields. CS=domain of rocks from the continental sector of Cameroon volcanic line (*blue color*); OS=domain of lavas from the oceanic sector of Cameroon volcanic line (*pink color*); ET=domain of undersaturated lavas from Mount Etinde. The different domains are according to Déruelle et al. (2007)

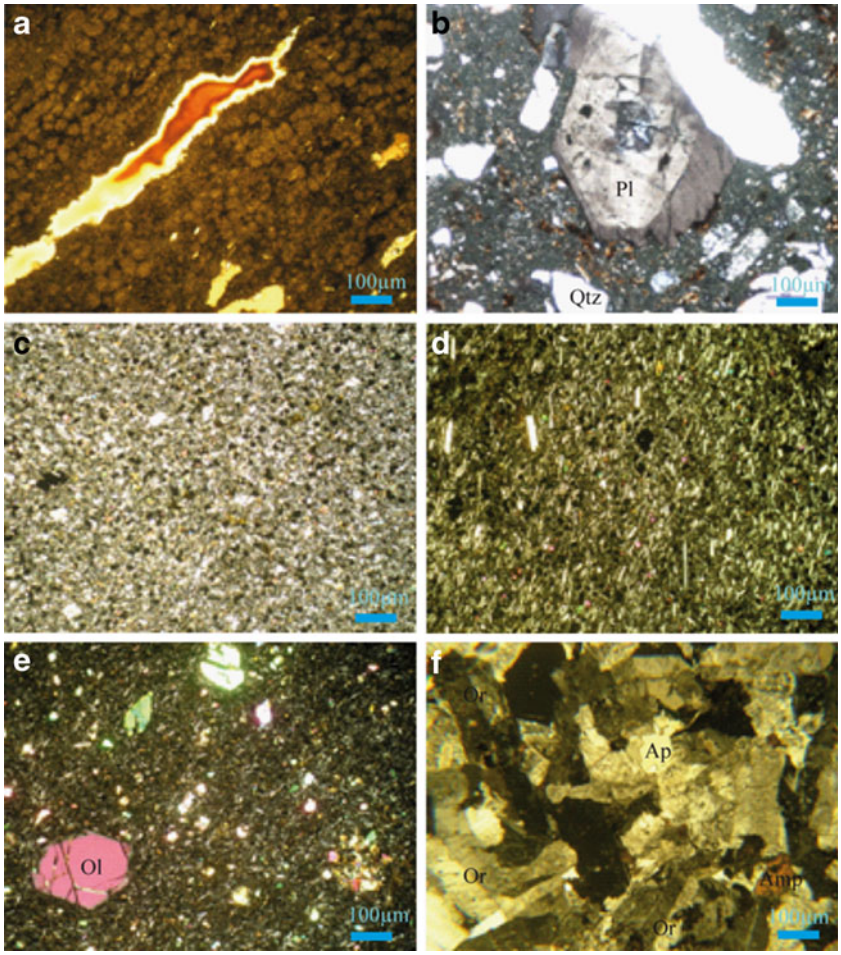

Fig. 3 Representative photomicrographs for the main recent magmatic rocks from Mbengwi. (**a**) Felsitic texture in a rhyolite F3; (**b**) brechitic texture in a rhyolitic tuff E52 showing a zoned plagioclase; (**c**) microlitic aphyritic texture in an hawaiite E50; (**d**) microlitic aphyritic texture in hawaiite E46 with plagioclase microlites showing a preferential orientation; (**e**) porphyritic basanite with olivine phenocrysts in a microlitic groundmass made up of sanidine olivine and opaque minerals; (**f**) equigranular texture in a quartz syenite. *Ap=apatite, Amp=amphibole, Pl=plagioclase, Ol=olivine, Or=orthoclase*

They have a fluidal structure marked by the orientation of microlites and vacuoles parallel to glass trails. Their groundmass is very finely crystallized, locally glassy and represents almost 85 % of the rock. The phenocryst phases comprise K-albite (6–8 %), Na-sanidine (≈4 %) and quartz (2 %).

Syenites and felsic lavas outcrop in metric blocks at the same place, meaning that they may be genetically associated. They have a fine-to medium-grained texture and are made up of amphibole (8–12 %), orthoclase and/or microcline, (29 %), sanidine (20–37 %) plagioclase (20–31 %), clinopyroxene (≈ 4 %), opaque minerals (≈ 2 %) and occasionally either quartz (2 %) or olivine (≈ 1.5 %), apatite (< 1 %), zircon (< 1 %) and titanite (< 1 %). The presence or lack of quartz, fayalite and pyroxene phenocrysts led us to distinguish two different types of syenites: the fayalite-pyroxene syenites, and the quartz-syenites. Microcline is secondary and orthoclase is perthitic and almost always zoned. Green hornblende is associated with pyroxene and located within spaces between phenocrysts or included in feldspar. Olivine and titanite are interstitial.

Mineral chemistry

Feldspars

Representative feldspars analyses from Mbengwi recent magmatic rocks are shown in Table 1. Plagioclase compositions range from labradorite ($An_{55.16–69.32}Ab_{29.28–42.91}Or_{1.1.28–3.11}$) to andesine ($An_{33.78–45.31}Ab_{51.01–61.12}Or_{3.20–8.02}$) in basanites, from labradorite ($An_{51.44–62.15}Ab_{36.25–43.70}Or_{1.53–3.58}$) to oligoclase ($An_{28.85–29.48}Ab_{63.97–64.69}Or_{6.46–6.56}$) in hawaiites whereas in mugearites plagioclase is labradorite ($An_{51.36}Ab_{46.95}Or_{1.70}$) and Na-albite ($An_{0.14–0.55}Ab_{64.10–67.60}Or_{32.23–35.33}$) in rhyolites and quartz-syenites ($An_{0–0.09}Ab_{95.35–99.23}Or_{0.73–4.65}$) (Fig. 4). Compositions are homogenous from the rim to the core of minerals. Alkali feldspars are mostly present in felsic rocks and scarce in mafic lavas. Their compositions are K-albite ($An_{5.04}Ab_{56.87}Or_{38.09}$) in hawaiites, K-albite ($An_{7.03–13.94}Ab_{66.28–70.99}Or_{16.96–18.76}$) and Na-sanidine ($An_{1.60}Ab_{60.76}Or_{37.60}$) in trachytes, K-albite ($An_{0.14–10.57}Ab_{64.10–72.19}Or_{15.88–35.33}$) and Na-sanidine($An_{0.64}Ab_{57.34}Or_{42.02}$) in rhyolites, K-albite

Table 1 Representative microprobe analyses of feldspars from the Mbengwi recent magmatic rocks

	Basanites				Hawaiites										Mugearite	Trachytes			Rhyolites				Quartz syenites		Fayalite syenites	
Sample	E30	E51	E51	E55	E146	E40	E40	E43	E46	E5	E50	E7	E7-1	E4	D15	E56	E56	E56	F3	F3	F2	F2	F0	F0	F1	F1
SiO_2	51.82	51.01	49.74	62.71	60.57	58.89	65.40	60.07	53.33	52.88	60.23	51.92	52.86	53.60	54.70	67.17	63.63	63.82	67.69	67.82	64.91	67.67	69.17	65.74	64.99	67.02
TiO_2	0.26	0.15	0.23	b.d.	0.16	0.18	0.47	b.d.	0.03	0.03	b.d.	0.26	0.34	0.15	0.31	0.10	0.07	b.d.	b.d.	b.d.	0.14	0.13	0.03	b.d.	0.2	0.13
Al_2O_3	29.98	30.96	31.26	23.53	24.43	25.12	19.50	24.90	29.30	28.43	24.34	29.14	29.6	28.72	27.45	18.74	21.26	21.32	18.35	18.24	20.72	17.97	19.41	18	20.48	18.27
Fe_2O_3	0.80	0.72	0.87	0.11	0.23	0.65	0.56	0.05	0.70	0.70	0.29	0.98	0.86	0.93	0.44	0.53	0.39	0.24	0.64	0.62	0.25	0.62	0.03	0.19	0.3	0.53
MgO	b.d.	b.d.	b.d.	b.d.	b.d.	b.d.	b.d.	b.d.	b.d.	b.d.	b.d.	b.d.	b.d.	b.d.	b.d.	b.d.	b.d.	b.d.	b.d.	b.d.	b.d.	b.d.	b.d.	b.d.	b.d.	b.d.
CaO	12.92	14.00	15.12	4.96	6.20	7.71	1.04	7.06	11.87	11.97	6.16	12.94	12.33	11.65	10.66	0.33	2.27	2.89	0.03	0.03	2.41	0.13	0.01	b.d.	2.11	b.d.
SrO	b.d.	b.d.	b.d.	b.d.	b.d.	b.d.	b.d.	b.d.	b.d.	b.d.	b.d.	b.d.	b.d.	b.d.	b.d.	b.d.	b.d.	b.d.	b.d.	b.d.	b.d.	b.d.	b.d.	b.d.	b.d.	b.d.
BaO	b.d.	b.d.	b.d.	b.d.	b.d.	b.d.	b.d.	b.d.	b.d.	b.d.	b.d.	0.03	0.05	b.d.	b.d.	0.02	0.62	0.56	b.d.	b.d.	0.15	b.d.	b.d.	0.16	0.41	b.d.
Na_2O	3.81	3.27	2.91	8.11	7.68	6.86	6.47	7.06	4.49	4.63	7.49	4.17	4.34	4.77	5.38	6.93	8.14	7.58	7.83	7.75	8.23	6.52	11.71	1.48	8.08	6.29
K_2O	0.39	0.24	0.24	0.93	1.17	0.99	6.59	0.89	0.37	0.40	1.41	0.27	0.26	0.29	0.30	6.52	2.96	3.27	5.81	5.85	2.75	7.27	0.13	14.18	3.35	7.7
Rb_2O	b.d.	b.d.	b.d.	b.d.	b.d.	b.d.	b.d.	b.d.	b.d.	b.d.	b.d.	b.d.	b.d.	b.d.	b.d.	b.d.	b.d.	b.d.	b.d.	b.d.	b.d.	b.d.	b.d.	b.d.	b.d.	b.d.
Sum (wt.%)	99.98	100.35	100.37	100.36	100.43	100.40	100.02	100.03	100.10	99.04	99.91	99.72	100.64	100.10	99.24	100.34	99.33	99.68	100.34	100.32	99.56	100.30	100.48	99.75	99.91	99.94
Si	2.36	2.32	2.27	2.77	2.70	2.64	2.94	2.68	2.42	2.43	2.70	2.37	2.39	2.43	2.49	2.99	2.86	2.86	3.01	3.02	2.90	3.02	3.01	3.02	2.90	3.01
Ti	0.01	0.01	0.01	b.d.	0.01	0.01	0.02	b.d.	0.00	0.00	b.d.	0.01	0.01	0.01	0.01	0.00	0.00	b.d.	b.d.	b.d.	0.01	0.00	0.00	b.d.	0.01	0.00
Al ^{IV}	1.61	1.66	1.68	1.23	1.28	1.33	1.03	1.31	1.56	1.54	1.29	1.57	1.58	1.53	1.47	0.99	1.13	1.13	0.96	0.96	1.09	0.95	0.99	0.98	1.08	0.97
Al ^{VI}	b.d.	b.d.	b.d.	b.d.	b.d.	b.d.	b.d.	b.d.	b.d.	b.d.	b.d.	b.d.	b.d.	b.d.	b.d.	b.d.	b.d.	b.d.	b.d.	b.d.	b.d.	b.d.	b.d.	b.d.	b.d.	b.d.
Fe^{3+}	0.03	0.03	0.03	0.00	0.01	0.02	0.02	0.00	0.02	0.02	0.01	0.03	0.03	0.03	0.02	0.02	0.01	0.01	0.02	0.02	0.01	0.02	0.00	0.01	0.01	0.02
Mg	b.d.	b.d.	b.d.	b.d.	b.d.	b.d.	b.d.	b.d.	b.d.	b.d.	b.d.	b.d.	b.d.	b.d.	b.d.	b.d.	b.d.	b.d.	b.d.	b.d.	b.d.	b.d.	b.d.	b.d.	b.d.	b.d.
Ca	0.63	0.68	0.74	0.24	0.30	0.37	0.05	0.34	0.58	0.59	0.30	0.63	0.60	0.57	0.52	0.02	0.11	0.14	0.00	0.00	0.12	0.01	b.d.	b.d.	0.10	b.d.
Sr	b.d.	b.d.	b.d.	b.d.	b.d.	b.d.	b.d.	b.d.	b.d.	b.d.	b.d.	b.d.	b.d.	b.d.	b.d.	b.d.	b.d.	b.d.	b.d.	b.d.	b.d.	b.d.	b.d.	b.d.	b.d.	b.d.
Ba	b.d.	b.d.	b.d.	b.d.	b.d.	b.d.	b.d.	b.d.	b.d.	b.d.	b.d.	0.00	0.00	b.d.	b.d.	b.d.	0.01	0.01	b.d.	b.d.	0.00	b.d.	b.d.	0.00	0.01	b.d.
Na	0.34	0.29	0.26	0.70	0.66	0.60	0.56	0.61	0.39	0.41	0.65	0.37	0.38	0.42	0.48	0.60	0.71	0.66	0.68	0.67	0.71	0.57	0.99	0.13	0.70	0.55
K	0.02	0.01	0.01	0.05	0.07	0.06	0.38	0.05	0.021	0.02	0.08	0.02	0.02	0.02	0.02	0.37	0.17	0.19	0.33	0.33	0.16	0.41	0.01	0.83	0.19	0.44
Rb	b.d.	b.d.	b.d.	b.d.	b.d.	b.d.	b.d.	b.d.	b.d.	b.d.	b.d.	b.d.	b.d.	b.d.	b.d.	b.d.	b.d.	b.d.	b.d.	b.d.	b.d.	b.d.	b.d.	b.d.	b.d.	b.d.
Sum Cations	4.99	4.99	5.00	4.99	5.02	5.01	4.99	4.99	5.00	5.01	5.02	5.00	5.00	5.00	5.00	4.99	5.00	4.99	5.00	5.00	4.99	4.98	4.99	4.97	4.99	4.99
Ab	34.03	29.28	25.49	70.74	64.69	58.26	56.87	61.12	39.76	40.24	63.38	36.25	38.27	41.86	46.95	60.76	71.00	66.28	67.11	66.72	72.19	57.34	99.23	13.65	70.08	55.40
An	63.69	69.32	73.13	23.92	28.85	36.19	5.04	33.79	58.10	57.49	28.78	62.15	60.10	56.47	51.36	1.60	10.95	13.94	0.15	0.14	11.66	0.65	0.05	b.d.	10.09	0.00
Or	2.29	1.408	1.38	5.34	6.46	5.55	38.09	5.10	2.14	2.27	7.84	1.54	1.53	1.67	1.70	37.60	16.96	18.79	32.74	33.14	15.88	42.02	0.73	86.05	19.11	44.60
Celsian	b.d.	b.d.	b.d.	b.d.	b.d.	b.d.	b.d.	b.d.	b.d.	b.d.	b.d.	0.05	0.09	b.d.	b.d.	0.04	1.09	0.99	b.d.	b.d.	0.27	b.d.	b.d.	0.30	0.72	b.d.
Rb-Feld	b.d.	b.d.	b.d.	b.d.	b.d.	b.d.	b.d.	b.d.	b.d.	b.d.	b.d.	b.d.	b.d.	b.d.	b.d.	b.d.	b.d.	b.d.	b.d.	b.d.	b.d.	b.d.	b.d.	b.d.	b.d.	b.d.
Sr-Feld	b.d.	b.d.	b.d.	b.d.	b.d.	b.d.	b.d.	b.d.	b.d.	b.d.	b.d.	b.d.	b.d.	b.d.	b.d.	b.d.	b.d.	b.d.	b.d.	b.d.	b.d.	b.d.	b.d.	b.d.	b.d.	b.d.

b.d. = below detection

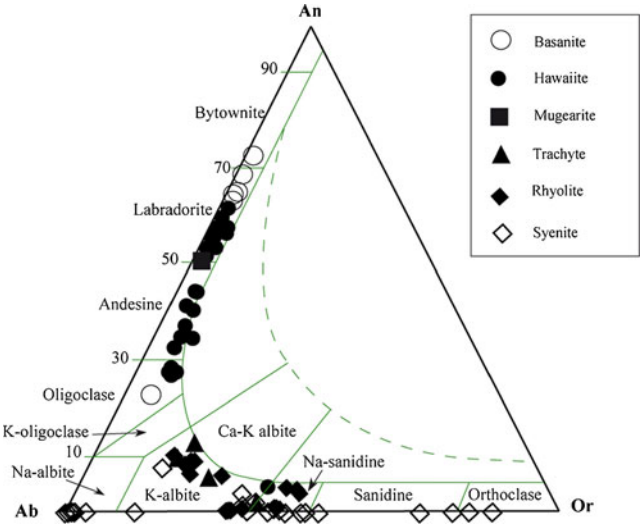

Fig. 4 Compositions of feldspars in the Ab-Or-An diagram from Smith and Brown (1988)

($An_{0.-10.09}Ab_{55.40-85.60}Or_{14.40-44.60}$), Na-sanidine ($An_{0-0.83}Ab_{51\cdot41-59.68}Or_{39.49-48.49}$), sanidine ($An_{0-0.08}Ab_{21.39-48.63}Or_{51.28-78.51}$), orthoclase and microcline ($An_0Ab_{13.65-14.85}Or_{81.78-86.05}$) in syenites. The zoning of alkali feldspars observed in syenites is marked by enrichment in K_2O and depletion in Na_2O and CaO from the core to the rim of crystals. These feldspars are all characterized by $Si+Al^{IV}<4$ and their contents in celsiane are negligible (< 0.7 wt.%).

Clinopyroxenes

Ca-rich pyroxenes occur both in lavas and syenites. Their composition (Table 2) shows a total absence of Cr_2O_3. Their Mg# (100.Mg/(Mg+Fe^t)) varies considerably from 29.60 in syenites to 85.00 in basanites. Al^{IV}/Al^{VI} ratios display a large range of variation from 0 in fayalite-pyroxene syenite to 35 in hawaiites E7. According to the classification scheme of Morimoto et al. (1988) (Fig. 5), clinopyroxenes have composition of diopside ($Wo_{45.10-51.40}En_{40.18-41.58}Fs_{7.35-14.72}$) and augite ($Wo_{42.28-44.96}En_{36.24-47.61}Fs_{8.42-21.47}$) in basanites, and of mainly diopside ($Wo_{46\cdot52-54.24}En_{34.17-43.76}Fs_{6.53-19.31}$) in hawaiites, augite ($Wo_{41.67-44.19}En_{27.30-33.26}Fs_{23.85-28.50}$) in trachytes and augite ($Wo_{43.45-43.92}En_{16.75-21.69}Fs_{34.39-39.80}$) and hedenbergite ($Wo_{45.40}En_{21.30}Fs_{33.30}$) in pyroxene fayalite-syenites. In almost all basanites samples and in some hawaiites having mantle xenocrysts, there are clinopyroxene phenocrysts with Wo contents >50 % which correspond to fassaites. This fassaitic character of some pyroxene is a common feature of pyroxenes from basaltic lavas from CVL which has already been pointed out the neighboring Bamenda basanites (Kamgang et al. 2008) and the Quaternary alkaline basalts of the Noun Plain, and of Mount Bambouto (Wandji et al. 2000; Kagou Dongmo et al. 2010). The Ti/Al ratio is in the range (0.04–2.18) and most of the lavas, except basanite, have an average close to 0.30 reflecting a relatively low equilibrium pressure (Wass 1979). There is a negative correlation of Si and Mn and Fe_{total} with Mg#, a positive one for Al_{total} and Ti and no correlation for Ca.

Amphiboles

Amphiboles (Table 3) are sodic-calcic and vary from katophorite to Fe-richterite (Fig. 6) following the classification scheme of Leake et al. (1997). They are characterized by a large range in Mg# [100 Mg/(Mg+Fe^{2+})] (0.40–28.20), low TiO_2 (≤ 1.80 wt.%) and MnO (0.78–1.66 wt.%) contents. Their SiO_2 and Al_2O_3 contents range from 45.44 to 49.97 wt.% and from 0.40 to 2.22 wt.% respectively, while the sum of alkali ranges from 2.90 to 7.8 wt.%. Richterite is characterized by lower MgO (0.06–4.02 wt.%), and CaO (2.37–7.09 wt.%) contents compared with katophorite (3.81–5.02 wt.% and 6.52–7.48 wt.% respectively). In contrast Al_2O_3 contents are higher in katophorite (1.91–2.22 wt.%) than in richterite (0.40–1.87 wt.%).

Olivines

Olivines have a composition of forsterite in mafic lavas and fayalite in syenites (Table 4). The crystals are generally chemically homogeneous, but they can sometimes be slightly zoned. The zoning is normal in basanites and marked by the increase of forsterite content from the cores to rims of crystals (e.g. Fo_{70} to Fo_{76} in E30), and inversely in hawaïtes (e.g. Fo_{87} to Fo_{83} in E7). In lavas, Mg-number [100 Mg/(Mg+Fe^{2*})] (60.59–89.11), CaO (0.09–0.59 wt.%), MnO (0.10–0.96 wt.%) and NiO (< 0.36 wt.%) contents of olivine are similar to those of other lavas from the CVL (Ngounouno et al. 2001; Wandji et al. 2009; Kagou Dongmo et al. 2010)

In pyroxene fayalite syenites, fayalite (Fa_{81-88}) is enriched in MnO (3.93–4.98 wt.%) relative to forsterite from mafic lavas. Their NiO (< 0.09 wt.%), CaO (0.33–0.45 wt.%) and Cr_2O_3 (< 0.07 wt.%) contents are rather low. FeO, MnO and CaO, are negatively correlated to the forsterite content while SiO_2 and TiO_2 positively correlate.

Opaque minerals

Opaque minerals have compositions of ilmenite (occurring only in quartz syenite) and spinels. According to the nomenclature of Haggerty and Tompkins (1983), spinels correspond to ulvospinel, magnetite and magnesioferrite (Fig. 7). Their TiO_2>0.20 wt.% and Fe^{2+}/Fe^{3+}<2 for almost all the samples, preclude their mantle origin according to Kamenetsky et al. (2001). They are characterized by Cr#

Table 2 Representative microprpobe analysis of pyroxenes from the Mbengwi recent magmatic rocks Fe^{2+} Fe3+ Al IV and Al VI have been estimated following the method described in Deer et al. (1992)

	Basanites									Hawaiites				Trachytes		fayalite Syenites		
Sample	E30	E30	E30	E30	E51	E51	E51	E55	E55	E146	E7	E7	E7-1	E56	E56	F1	F1	F1
SiO_2	44.53	47.23	51.44	45.84	48.88	46.43	46.79	49.90	47.02	51.86	49.30	43.45	49.54	51.24	51.17	50.12	49.65	49.25
TiO_2	3.79	3.25	0.68	2.97	1.49	2.44	2.14	2.00	2.22	0.16	1.89	4.27	1.32	0.56	0.68	0.57	0.63	0.54
Al_2O_3	10.67	5.69	6.36	8.77	6.24	9.21	9.00	12.38	9.23	2.08	4.13	8.84	6.83	1.04	1.34	0.37	0.42	0.39
Cr_2O_3	0.10	0.01	0.73	0.06	b.d.	0.03	0.07	b.d.	0.02	b.d.	0.18	0.06	0.16	0.02	b.d.	b.d.	b.d.	b.d.
Fe_2O_3(c)	3.18	2.63	b.d.	3.44	2.86	b.d.	0.29	b.d.	1.45	0.80	3.06	4.26	b.d.	0.21	0.48	1.23	2.50	2.62
FeO(c)	3.87	5.06	4.84	4.43	6.91	8.45	7.52	5.01	6.16	11.6	3.84	4.49	6.69	15.31	13.94	19.50	19.21	18.35
MnO	0.07	0.12	0.07	0.01	0.16	0.05	0.11	0.12	0.13	0.21	0.20	0.13	0.17	1.19	1.14	1.75	1.87	1.54
MgO	12.29	13.24	15.37	12.32	13.93	12.94	13.26	10.3	13.02	11.52	14.43	11.12	13.87	10.54	10.91	6.65	6.80	6.58
CaO	20.99	22.78	19.75	21.79	18.51	20.20	20.78	18.69	20.46	21.82	22.81	22.49	22.10	19.02	19.56	18.93	19.15	19.53
Na_2O	0.83	0.30	0.97	0.68	0.87	b.d.	b.d.	2.01	0.54	0.39	0.36	0.55	b.d.	0.44	0.45	0.61	0.44	0.58
K_2O	0.02	0.02	b.d.	b.d.	0.05	b.d.	b.d.	0.13	b.d.	0.01	b.d.	b.d.	b.d.	0.02	0.04	0.07	0.04	b.d.
Sum (wt.%)	100.33	100.32	100.21	100.32	99.90	99.74	99.95	100.54	100.26	100.45	100.19	99.65	100.69	99.59	99.71	99.81	100.70	99.39
Si	1.65	1.76	1.87	1.70	1.81	1.73	1.74	1.80	1.74	1.95	1.83	1.64	1.82	1.97	1.96	1.98	1.95	1.96
Ti	0.11	0.09	0.02	0.08	0.04	0.07	0.06	0.05	0.06	0.00	0.05	0.12	0.04	0.02	0.02	0.02	0.02	0.02
Al^{IV}	0.35	0.24	0.13	0.30	0.19	0.27	0.26	0.20	0.26	0.05	0.18	0.36	0.18	0.03	0.04	0.02	0.02	0.02
Al^{VI}	0.11	0.01	0.14	0.09	0.09	0.14	0.13	0.33	0.14	0.05	0.01	0.03	0.11	0.02	0.02	b.d.	b.d.	b.d.
Cr	0.00	b.d.	0.02	0.00	b.d.	0.00	0.00	b.d.	0.00	b.d.	0.01	0.00	0.01	0.00	b.d.	b.d.	b.d.	b.d.
Fe^{3+}	0.09	0.07	b.d.	0.10	0.08	b.d.	0.01	b.d.	0.04	0.02	0.09	0.12	b.d.	0.01	0.01	0.04	0.07	0.08
Fe^{2+}	0.12	0.16	0.15	0.14	0.22	0.26	0.23	0.15	0.19	0.37	0.12	0.14	0.21	0.49	0.45	0.65	0.63	0.61
Mn^{2+}	0.00	0.00	0.00	b.d.	0.01	0.00	0.00	0.00	0.00	0.01	0.01	0.00	0.01	0.04	0.04	0.06	0.06	0.05
Mg	0.68	0.74	0.83	0.68	0.77	0.72	0.73	0.55	0.72	0.65	0.80	0.63	0.76	0.61	0.62	0.39	0.40	0.39
Ca	0.83	0.91	0.77	0.87	0.74	0.81	0.83	0.72	0.81	0.88	0.91	0.91	0.87	0.79	0.80	0.80	0.81	0.83
Na	0.06	0.02	0.09	0.05	0.06	b.d.	b.d.	0.14	0.04	0.03	0.03	0.04	b.d.	0.03	0.03	0.05	0.03	0.05
K	0.00	0.00	b.d.	b.d.	0.00	b.d.	b.d.	0.01	b.d.	0.00	b.d.	b.d.	b.d.	0.00	0.00	0.00	0.00	0
Sum Cation	4.00	4.00	4.00	4.00	4.00	4.00	4.00	3.96	4.00	4.00	4.00	4.00	4.00	4.00	4.00	4.00	4.00	4.00
Wo(Ca)	51.07	50.45	43.97	51.40	42.76	45.10	46.07	50.62	47.16	46.52	49.71	54.24	47.40	41.67	42.89	43.62	43.92	45.40
En(Mg)	41.59	40.81	47.61	40.44	44.78	40.18	40.92	38.80	41.75	34.18	43.76	37.32	41.39	32.14	33.27	21.31	21.69	21.30
Fs(Fe^{2+})	7.35	8.74	8.42	8.16	12.46	14.72	13.01	10.59	11.09	19.31	6.53	8.44	11.21	26.19	23.85	35.07	34.39	33.30
XMg	0.85	0.82	0.85	0.83	0.78	0.73	0.76	0.79	0.79	0.64	0.87	0.82	0.79	0.55	0.58	0.38	0.39	0.39

(c)=calculated b.d. = below detection

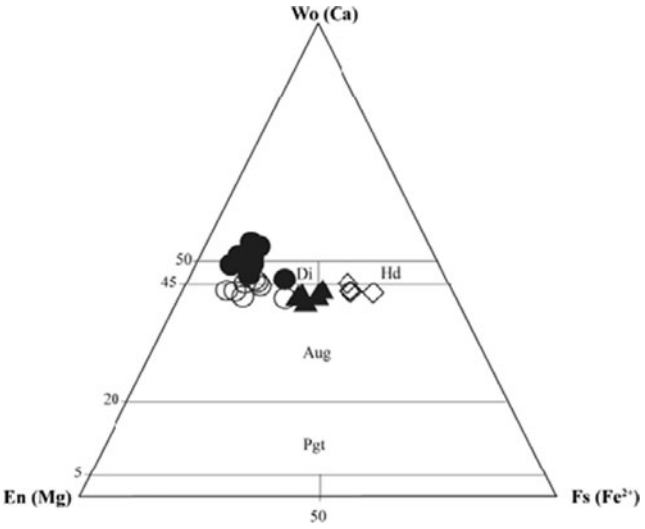

Fig. 5 En–Wo—Fe ternary diagram of pyroxenes (Morimoto et al. 1988) *Di=Diopside; Pgt=Pigeonite; Aug=Augite; Wo=Wollastonite; En=Enstatite; Fs=ferrosilite. Pyroxene having Wo content >50 wt% are fassaite*

(100Cr/(Cr+Al))≤38.63; Y_{Fe3+} (100 $Fe^{3+}/(Fe^{3+}$ + Cr+Al)) ranging from 13.92 to 96.18; $Fe^{2+\#}$ (100 $Fe^{2+}/(Fe^{2+}$ + Mg)) from 38.74 to 88.96. Finally their $Mg^{\#}$ (Fe_{total}) ratios vary from 11.03 to 61.26. Basanites contain the most magnesian (Mg#=61.26), chromiferous (Cr#=35.98–38.63), aluminous (Al_2O_3=51.70–52.73 wt.%), and NiO-rich (0.17 wt.%) spinels.

Carbonates

Carbonates include siderite, magnesite and rarely ankerite. Their rhodochrosite contents are less than 5.3 wt.%. According to the geothermometer of Davidson (1994) their crystallization temperatures range from 730 °C for ankerite to 525 °C for siderite and magnesite.

Whole rock geochemistry

Major and trace element compositions of 18 representative samples of the Mbengwi area are presented in Table 5. These results were recomputed on an anhydrous base because the loss on ignition contents was higher than the critical value of 2 wt.% in almost 30 % of samples.

Major elements

The Mbengwi recent volcanic rocks form a bimodal alkaline suite from basanites to rhyolites, with a compositional "Daly gap" between mafic and felsic terms as observed for the most of the CVL massifs. SiO_2 varies from 42.89 to 76.00 wt.% with a gap between 49.86 and 62.63 wt.%. The sum of alkali (Na_2O+K_2O) varies from 3.47 to 11.73 wt.% and Na_2O/K_2O ratios from 1.01 to 5.53. The mafic rocks are sodic (Na_2O/K_2O: 1.57–5.53) except the basanite sample E30 (Na_2O/K_2O=1.6), and have moderate MgO contents (4.2–11.2 wt.%). The felsic lavas are essentially sodi-potassic (Na_2O/K_2O: 1.01–1.25), slightly metaluminous to peralkaline. Rhyolites and trachytes are commenditic. These features are similar to those of some recent lavas from the continental sector of CVL such as lavas from Mounts Bamenda (Kamgang et al. 2007; 2008), Manengouba (Kagou Dongmo et al. 2001) and the Noun (Wandji 1995) and Tombel (Nkouathio 1997) plains and to those of Hawaiian lavas (Macdonald and Katsura 1964).

In syenites, the SiO_2, Al_2O_3 and MgO contents range from 63.44 to 64.81 wt.%, 15.34 to 16.71 wt.% and 0.40 to 0.50 wt.% respectively. Syenites are rich in alkali (Na_2O+K_2O=11.46–11.60 wt.%) and characterized by a low Mg# (7.5–11.5), and low Ni contents< 5 ppm. Their molar ratios K_2O/Na_2O (0.54–0.61), [(Na_2O+K_2O)/Al_2O_3: 0.95–1.03], and CaO/Al_2O_3<1 are similar to those of the Nda Ali syenites from CVL (Njonfang and Moreau 1996) and Kerguelen Islands syenites (Giret 1983). The quartz-syenite sample (F0) is peralkaline according to its peralkalinity index [(Na_2O+K_2O)/Al_2O_3>1], while fayalite syenites are weakly metaluminous with (Na_2O+K_2O)/Al_2O_3 ratios ranging between 0.95 and 0.97. The fayalite-pyroxene syenites are earlier than quartz syenites. This assertion is mineralogically attested both by early crystallized mineral such as olivine in the fayalite-pyroxene syenite and by the presence of late crystallized mineral such as magmatic zircon in quartz-syenites. Otherwise the highest Zr contents of quartz-syenites (979 ppm) compared to fayalite-pyroxene syenites (325 ppm) suggest that the peralkaline quartz-syenite are more evolved, therefore later than fayalite-pyroxene syenites.

The Mbengwi recent magmatic rocks have a differentiation index (DI) ranging from 22.2 to 89.7 in lavas and 84.7 to 86.2 in syenites. All the rocks are apatite (0.09–4.40 wt.%) and ilmenite (0.65 to 8.36 wt.%) normative.

Felsic rocks are diopside (4.53–5.13 wt.%) and hypersthene (0.97–7.29 wt.%) normative, while mafic lavas contain normative magnetite (2.13–2.62 wt.%) and nepheline (1.48–22.45 wt.%) despite the absence of modal nepheline. Normative acmite (2.01–2.79 wt.%) is present only in peralkaline rocks (quartz syenites and rhyolites) and normative sodium metasilicate (≤ 0.97 wt.%) in rhyolites.

In the Harker diagrams (Fig. 8a), there is a continuous decrease in MgO, Fe_2O_3, CaO, and TiO_2 with increasing of the differentiation index (DI), while K_2O and obviously

Table 3 Representative microprobe analyses of amphibole from the Mbengwi syenites

	Quartz Syenites											Fayalite syenites					
Sample	F0	F0	F0	F0	F0	F0	F0	F0	F0	F0	F0	F1	F1	F1	F1	F1	F1
SiO_2	45.44	49.97	48.58	48.62	48.27	48.41	47.51	47.47	47.62	47.6	47.56	47.4	48.37	48.19	47.2	47.33	47.38
TiO_2	0.08	b.d.	1.18	0.79	1.10	1.40	0.94	1.76	1.19	1.34	1.42	1.55	1.65	1.84	1.50	1.82	1.67
Al_2O_3	0.63	0.40	1.23	1.17	1.04	0.91	0.91	1.62	2.08	2.22	2.18	1.91	1.84	1.87	1.26	1.30	1.33
Cr_2O_3	b.d.	0.02	b.d.	0.06	0.01	0.08	b.d.	0.03	b.d.	0.15	0.04	b.d.	b.d.	b.d.	b.d.	0.06	b.d.
Fe_2O_3(c)	12.26	6.92	6.69	10.51	4.16	7.94	5.24	0.58	4.52	5.80	5.57	5.57	2.67	3.14	6.62	6.28	6.32
FeO(c)	25.87	29.26	23.96	23.92	27.52	27.11	28.84	30.48	24.38	23.00	23.20	25.21	27.08	25.94	28.88	29.30	29.19
MnO	1.66	1.53	1.17	1.52	1.50	1.60	1.38	1.17	0.78	1.14	0.98	1.16	1.26	1.26	1.47	1.44	1.46
MgO	0.06	0.37	3.93	1.97	2.40	0.28	0.47	2.37	5.02	4.87	5.10	3.81	3.62	4.02	0.78	0.61	0.52
CaO	6.50	7.09	4.86	2.36	5.11	2.37	3.22	6.52	7.48	6.90	7.21	6.20	6.34	6.45	4.79	4.74	4.69
Na_2O	2.78	2.51	5.23	6.82	5.13	6.38	6.38	4.96	3.81	3.98	3.88	4.66	4.79	4.44	5.33	5.29	5.27
K_2O	0.49	0.40	1.14	1.02	1.30	0.99	0.95	1.05	0.99	0.88	0.92	1.11	1.11	1.09	1.13	1.18	1.14
ZrO_2	b.d.	b.d.	b.d.	b.d.	b.d.	b.d.	b.d.	b.d.	b.d.	b.d.	b.d.	b.d.	b.d.	b.d.	b.d.	b.d.	b.d.
NiO	0.01	0.06	b.d.	b.d.	b.d.	0.11	0.05	b.d.	b.d.	b.d.	0.07	b.d.	0.12	b.d.	b.d.	b.d.	0.09
F	0.16	0.13	1.80	1.03	1.92	1.27	0.91	1.83	1.78	2.12	1.25	2.13	2.62	2.35	1.52	1.59	1.34
Cl	0.01	0.06	0.10	0.09	0.08	0.03	0.08	0.09	0.06	0.03	0.07	0.07	0.03	0.06	0.07	0.07	0.09
H_2O(c)	1.73	1.82	1.03	1.40	0.95	1.26	1.37	0.98	1.05	0.90	1.31	0.88	0.67	0.78	1.14	1.11	1.22
O=F	0.07	0.05	0.76	0.43	0.81	0.54	0.39	0.77	0.75	0.89	0.53	0.90	1.10	0.99	0.64	0.67	0.57
O=Cl	b.d	0.01	0.02	0.02	0.02	0.01	0.02	0.02	0.01	0.01	0.02	0.02	0.01	0.01	0.01	0.02	0.02
Sum wt.%	97.61	100.46	100.13	100.81	99.66	99.59	97.84	100.12	99.99	100.03	100.22	100.75	101.05	100.42	101.04	101.43	101.12
Si	7.52	7.92	7.62	7.64	7.72	7.761	7.79	7.60	7.47	7.44	7.42	7.45	7.58	7.56	7.54	7.54	7.56
Ti	0.01	b.d	0.14	0.09	0.13	0.17	0.12	0.21	0.14	0.16	0.17	0.18	0.19	0.22	0.18	0.22	0.20
Al^{IV}	0.12	0.08	0.23	0.22	0.20	0.17	0.18	0.31	0.38	0.41	0.40	0.35	0.34	0.35	0.24	0.24	0.25
Al^{VI}	b.d.	b.d.	b.d.	b.d.	b.d.	b.d.	b.d.	b.d.	b.d.	b.d.	b.d.	b.d.	b.d.	b.d.	b.d.	b.d.	b.d.
Cr	b.d.	0.00	b.d.	0.01	0.00	0.01	b.d.	0.00	b.d.	0.02	0.01	b.d.	b.d.	b.d.	b.d.	b.d.	b.d.
Fe^{3+}	1.53	0.83	0.79	1.24	0.5	0.96	0.65	0.07	0.53	0.68	0.65	0.66	0.32	0.37	0.80	0.75	0.80
Fe^{2+}	3.58	3.89	3.14	3.14	3.68	3.63	3.96	4.08	3.20	3.01	3.03	3.31	3.55	3.40	3.86	3.90	3.90
Mn^{2+}	0.23	0.21	0.16	0.20	0.20	0.22	0.19	0.16	0.10	0.15	0.13	0.15	0.17	0.17	0.20	0.20	0.20
Mg	0.02	0.09	0.92	0.46	0.57	0.07	0.11	0.56	1.17	1.13	1.19	0.89	0.85	0.94	0.19	0.15	0.12
Ca	1.15	1.20	0.82	0.40	0.88	0.41	0.57	1.12	1.26	1.16	1.21	1.04	1.06	1.08	0.82	0.81	0.80
Na	0.89	0.77	1.59	2.08	1.59	1.98	2.03	1.54	1.16	1.21	1.17	1.42	1.45	1.35	1.65	1.63	1.63
K	0.10	0.08	0.23	0.20	0.27	0.20	0.20	0.22	0.20	0.18	0.18	0.22	0.22	0.22	0.23	0.24	0.23
Zr	b.d.	b.d.	b.d.	b.d.	b.d.	b.d.	b.d.	b.d.	b.d.	b.d.	b.d.	b.d.	b.d.	b.d.	b.d.	b.d.	b.d.
Ni	0.00	0.01	b.d.	b.d.	b.d.	0.01	0.01	b.d.	b.d.	b.d.	0.01	b.d.	0.01	b.d.	b.d.	b.d.	0.01
F	0.09	0.06	0.89	0.51	0.97	0.65	0.48	0.93	0.88	1.05	0.62	1.06	1.30	1.17	0.77	0.80	0.68
Cl	0.00	0.02	0.03	0.02	0.02	0.01	0.02	0.02	0.02	0.01	0.02	0.02	0.01	0.02	0.02	0.02	0.03
OH	1.91	1.92	1.08	1.46	1.01	1.35	1.50	1.05	1.10	0.94	1.36	0.92	0.70	0.82	1.21	1.18	1.30
Sum Cations	17.15	17.06	17.64	17.68	17.73	17.59	17.79	17.87	17.61	17.54	17.56	17.69	17.74	17.65	17.70	17.68	17.67
XMg	0.00	0.02	0.23	0.13	0.14	0.02	0.03	0.12	0.27	0.27	0.28	0.21	0.19	0.22	0.05	0.04	0.03

(c)=calculated b.d. = below detection

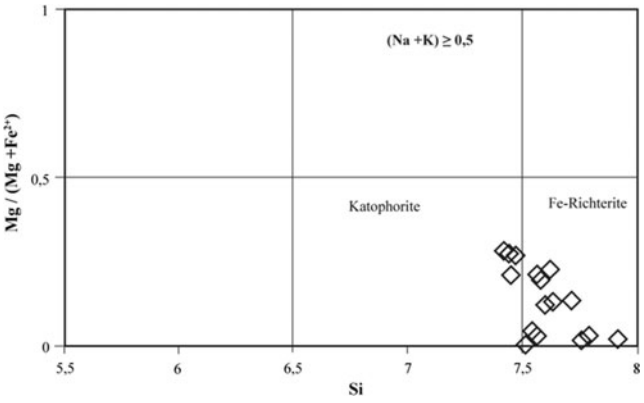

Fig. 6 Amphibole in Mg/(Mg+Fe^{2+}) vs Si (a.p.f.u) diagram, following the terminology of Leake et al. (1997)

SiO_2 increase from mafic to felsic rocks. In contrast, Al_2O_3 and MnO increase with DI in mafic lavas and decrease in felsic rocks. Overall, the Mbengwi lavas display major element variations similar to those from the Bamenda (Kamgang et al. 2007; 2008; 2010), Bambouto and Oku Mountains (Marzoli et al. 1999; 2000).

Trace elements

The amounts of Ni, Cu, Zn, Y, Ga, Pb and Sn vary considerably from mafic to felsic rocks. Ni (0.2–179.3 ppm with the highest value in the basanite E30), Cu (≤ 52.3 ppm with maximum in hawaiite E7-1), Sn (1.5–8.1 ppm with maximum in rhyolite), Zn (63.4–460 ppm with maximum in syenite BA83), Pb (1.6–14.ppm, with the highest content in syenite BA83), Y (21.4–97.9 ppm with the highest content in syenite BA83). The variation of incompatible trace elements is marked by the increase of Zr, Rb, Nb and Th from mafic to felsic rocks. The distribution of selected trace elements relative to Th contents is shown in figure 8b. The Rb contents are significantly higher in felsic rocks than in the mafic lavas. Zr, Nb, Rb, Y, Yb, La and Ta show a positive correlation with Th contents with a linear trend for Nb and Zr, contrary to Sr and V. The Sr contents decrease from mafic lavas (1241.6–790.7 ppm) to felsic rocks (< 236 ppm).

Zr/Rb (5.25–16.87) and Ga/Rb (0.32–1.04) ratios are nearly identical to those of the lavas from Bamenda Mountains (8.42–15.33 and 0.36–0.68 respectively) (Kamgang et al. 2007, 2008) and reflect an enrichment in Ga and high field strength elements (HFSE) relative to large-ion lithophile elements (LILE). The Zr/Nb ratios are almost constant for the entire series and range between 3.5 and 6.6, while Ba/Ta ratios range between 1.6 and 645.4. The Chondrite-normalized multi-element diagrams (Fig. 9a–b) show an enrichment from Ba to Ta (200–600 times the chondrite values) (McDonough and Sun. 1995) with the highest peaks at Nb and Ta. All spectra exhibit a negative Rb anomaly. This distribution in trace elements is comparable with those of oceanic island basalts (OIB).

The chondrite normalized rare earth elements patterns of mafic and felsic rocks are homogeneous and almost parallel (Fig. 10a–b). They show a strong enrichment in light rare-earth elements (LREE) compared with heavy rare-earth elements (HREE) $(La/Yb)_N$ (9.3–30). The values of Eu anomalies $[Eu/Eu^*=Eu_N/(Sm_N\ Gd_N)^{1/2}]$ as defined by Taylor and McLennan (1985) range from 1.13 to 0.96 in mafic rocks, and from 2.04 to 0.23 in felsic rocks. The mafic lavas show an overall weak negative Sm anomaly and a very slight positive Eu anomaly. In felsic rocks, positive anomalies (2.04–1.39) characterize metaluminous felsic rocks (trachytes and fayalite-pyroxene syenites) whereas negative Eu anomalies (0.66–0.23) mark peralkaline felsic rocks (rhyolites and quartz-syenites).

Isotopes

Ten new Rb/Sr and Sm/Nd isotopic ratio were obtained both in felsic (trachyte, rhyolite, fayalite-pyroxene syenite and quartz-syenite) and mafic rocks (basanite and hawaiite). The $^{87}Sr/^{86}Sr$ isotopic ratios vary between 0.703175 (Hawaiite E7-1) and 0.727181 (rhyolite) while $^{143}Nd/^{144}Nd$ ratios vary from 0.512691 (rhyolites and fayalite syenite) to 0.512903 (hawaiite). $^{87}Rb/^{86}Sr$ ratios remain low (< 0.2) in mafic lavas whereas in felsic rocks they are higher (0.5–63). The Sm/Nd ratios are low (0.11–0.13). The Rb/Sr whole rock isochrone yields an age of 28.2 Ma (Upper Eocene) for these magmatic formations; this age is almost similar to the 27.40± 0.6 MaK/Ar age recently obtained in a trachyte from Bamenda mountains (Kamgang et al. 2010).

Initial isotopic ratios range from 0.7017 to 0.7043 and from 0.5127 to 0.5129 for ($^{87}Sr/^{86}Sr$)i and ($^{143}Nd/^{144}Nd$)i respectively. The exceptionally high Sr isotopic ratio (0.72718) measured for the sample F3 (rhyolite) is due both to its high Rb content (138.97 ppm) and high Rb/Sr ratio. The radiogenic Sr ratio [$(^{87}Sr/^{86}Sr)_i$=070167] of the same rhyolite is an artifact, certainly overcorrected; however this sample belongs to the same magmatic history with other lavas according to its ($^{143}Nd/^{144}Nd$)i (0.5126685).

Discussion

Differentiation processes

Geochemical criteria favor fractional crystallization as the main process responsible of the range of composition and

Table 4 Representative microprobe analyses of olivines from the Mbengwi recent magmatic rocks

	Basanites				Hawaiites												Mugearites			Fayalite Syenites				
Sample	E30	E30	E51	E55	E146	E40	E43	E46	E5	E50	E50	E7	E7	E7-1	E7-1	E4	D15	D15	D15	F1	F1	F1	F1	F1
SiO_2	41.00	39.94	38.10	40.39	36.35	36.91	37.04	36.74	37.04	37.00	35.96	40.17	39.75	40.81	40.81	37.01	35.53	36.72	37.13	31.14	31.17	30.68	30.78	31.18
TiO_2	b.d.	b.d.	0.18	b.d.	0.04	0.05	0.08	0.08	b.d.	0.18	0.02	b.d.	b.d.	b.d.	b.d.	0.02	0.01	b.d.	0.03	0.06	0.07	0.07	0.08	0.03
Al_2O_3	b.d.	b.d.	b.d.	b.d.	b.d.	0.02	b.d.	b.d.	b.d.	0.12	b.d.	b.d.	b.d.	b.d.	b.d.	b.d.	b.d.	b.d.	0	0	0	0	0	0
Cr_2O_3	b.d.	0.02	0.05	0.02	b.d.	0.08	b.d.	0.02	b.d.	b.d.	0.04	0.02	0.03	0.02	0.06	b.d.	0.03	b.d.	0	0	0	0.04	0.07	0
FeO	10.47	17.10	27.54	15.34	30.63	29.58	28.57	29.08	27.43	31.01	33.63	14.63	16.00	12.23	12.59	30.81	33.96	29.64	29.54	57.42	57.57	59.75	57.87	57.47
MnO	0.13	0.27	0.45	0.25	0.92	0.67	0.71	0.72	0.67	0.82	0.96	0.24	0.19	0.12	0.12	0.76	0.78	0.52	0.58	4.18	3.93	4.98	4.46	4.35
MgO	48.08	42.88	34.03	44.27	32.02	33.00	33.05	33.01	34.81	28.84	29.13	44.99	44.29	47.42	46.92	30.97	29.94	33.50	33.04	7.52	7.07	4.79	6.74	6.67
CaO	0.09	0.19	0.46	0.22	0.37	0.38	0.35	0.41	0.34	0.59	0.37	0.13	0.23	0.23	0.24	0.42	0.26	0.15	0.21	0.33	0.37	0.44	0.45	0.43
NiO	0.28	0.27	0.13	0.19	b.d.	b.d.	b.d.	b.d.	b.d.	b.d.	b.d.	0.35	0.26	0.24	0.23	0.03	b.d.	b.d.	0.01	0.04	0.01	0.07	0.08	0
Sum (wt%)	100.04	100.67	100.94	100.67	100.33	100.69	99.80	100.06	100.29	98.57	100.12	100.53	100.75	101.08	100.97	100.02	100.51	100.53	100.54	100.69	100.20	100.82	100.53	100.13
Si	1.01	1.01	1.01	1.01	0.99	0.99	1.00	0.99	0.99	1.02	0.99	1.00	1.00	1.00	1.00	1.01	0.98	0.99	1.00	0.99	0.99	0.99	0.99	1.00
Ti	b.d.	b.d.	0.00	b.d.	0.00	0.00	0.00	0.00	b.d	0.00	0.00	b.d.	b.d.	b.d.	b.d.	b.d.	b.d.	b.d.	0.00	0.00	0.00	0.00	0.00	0.00
Al^{IV}	b.d.	b.d.	b.d.	b.d.	b.d.	0.00	b.d.	b.d.	b.d.	0.00	b.d.	b.d.	b.d.	b.d.	b.d.	b.d.	b.d.	b.d.	0	0	0	0	0	0
Al^{VI}	b.d.	b.d.	b.d.	b.d.	b.d.	b.d	b.d.	b.d.	b.d.	b.d.	b.d.	b.d.	b.d.	b.d.	b.d.	b.d.	b.d.	b.d.	0	0	0	0	0	0
Cr	b.d.	b.d.	0.00	b.d.	b.d.	0.00	b.d.	b.d.	b.d.	b.d.	0.001	b.d.	0.001	b.d.	0.00	b.d.	0.00	b.d.	0	0	0	0.00	0.00	0
Fe^{2+}	0.21	0.36	0.61	0.32	0.67	0.66	0.64	0.66	0.61	0.72	0.78	0.30	0.34	0.25	0.23	0.70	0.78	0.68	0.66	1.53	1.54	1.62	1.55	1.54
Mn^{2+}	0.00	0.01	0.01	0.01	0.02	0.02	0.02	0.02	0.02	0.02	0.02	0.01	0.00	0.00	0.00	0.02	0.02	0.01	0.01	0.11	0.11	0.14	0.12	0.12
Mg	1.76	1.61	1.34	1.65	1.30	1.32	1.33	1.33	1.39	1.19	1.20	1.67	1.65	1.73	1.72	1.25	1.23	1.34	1.32	0.36	0.34	0.23	0.32	0.32
Ca	0.00	0.01	0.01	0.01	0.01	0.01	0.01	0.01	0.01	0.02	0.01	0.00	0.01	0.01	0.01	0.01	0.01	0.00	0.01	0.01	0.01	0.02	0.02	0.015
Ni	0.01	0.01	0.00	0.00	b.d.	b.d.	b.d.	b.d.	b.d.	b.d.	b.d.	0.01	0.01	0.01	0.01	0.00	b.d.	b.d.	0	0.00	0	0.00	0.00	0
Sum Cations	2.99	2.99	2.99	2.99	3.01	3.00	3.00	3.00	3.01	2.97	3.00	3.00	3.00	3.00	3.00	2.99	3.02	3.01	3.00	3.00	3.00	3.00	3.00	3.00
Fa	0.11	0.18	0.31	0.16	0.35	0.33	0.33	0.33	0.31	0.38	0.39	0.15	0.17	0.13	0.13	0.36	0.39	0.33	0.33	0.81	0.82	0.88	0.83	0.83
Fo	0.89	0.82	0.69	0.84	0.65	0.67	0.67	0.67	0.69	0.62	0.61	0.85	0.83	0.87	0.87	0.64	0.61	0.67	0.67	0.19	0.18	0.12	0.17	0.17

b.d. = below detection

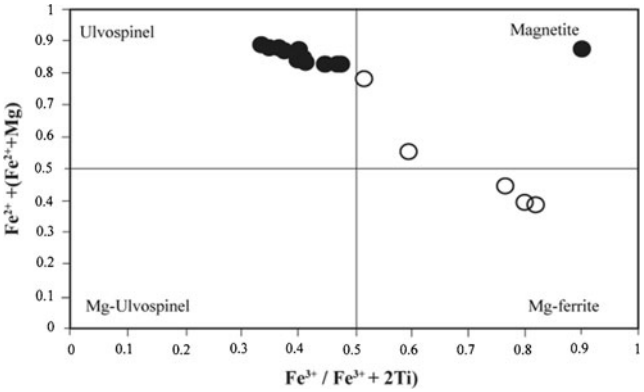

Fig. 7 Composition of opaque minerals after Haggerty and Tompkins (1983)

lithology of the Mbengwi recent magmatic formations. This evolution of the investigated rocks by fractional crystallization is emphasized by: i) the enrichment in LREE expressed by high La_N/Yb_N (8.7–22.6) ratios; ii) the parallelism observed between the REE patterns; iii) the homogeneity of various ratios of some hygromagmatophile elements such as Zr/Nb (3.51–6.61), Th/Hf (0.68–1.52) and La/Ta (8.4–16.23); iv) the distribution of some incompatible elements such as Th, Rb, Zr Hf and La defining positive evolution trends; vi) the decrease of compatible trace elements (Cr, Ni) with the increase of Rb and finally, vii) the constancy of La/Nb ratio with the increase of MgO contents (not shown). The low magnesium (MgO<5 wt.%), nickel (Ni<15.3 ppm) and chromium (Cr<4 ppm) contents of most hawaiites suggest a strong fractionation of olivine, clinopyroxene and Fe-Ti-oxide in the genesis of the Mbengwi mafic lavas. The strong negative Sr and Ti anomalies observed in the Mbengwi felsic rocks indicate that the fractionation of phases including plagioclase and Fe–Ti oxides were involved in the differentiation processes. The decrease of Ba contents while Zr contents increase points to the role of fractionation of alkali feldspar for the felsic rocks. The negative Eu anomaly of peralkaline quartz-syenites would be related to the fractionation of alkali feldspars; whereas the positive anomaly observed for fayalite-pyroxene syenites and trachytes is to be linked to the presence of plagioclase cumulative crystals before the magma solidification (Hanson 1980). The wide range of Ba and Sr in syenites within a fairly narrow interval of MgO content also suggests an accumulation of feldspar in the syenitic magma (Litvinovsky et al. 2002). The LREE enrichment could mean that these alkaline rocks have evolved by fractional crystallization at low pressure (Duchesne and Demaiffe 1978).

Using Rb vs. Sr diagram (Fig. 11) and Gd/Yb vs. La/Yb diagram (Fig. 12) for the Mbengwi less evolved samples (basanites) together with calculated curves for partial melting of lherzolites (Yokoyama et al. 2007) that have different mineral assemblages but have a chemically homogeneous composition (primitive mantle: Sun and McDonough, 1989), we notice that the Mbengwi rocks display two trends of fractional crystallization and were generated from at least two different melting sources.

In order to model the fractional crystallization, we used Gd/Y ratio and Zr contents (Fig. 13). Fractional crystallization was computed following Nonnotte et al. (2011). Typically 35 % of removed solid is needed to explain the chemical evolution from basanite (E30) to trachyte (E56). However it is worth mentioning that basanites display a large range of trace element signatures. Each basanite is a product of partial melting. Therefore, we have used the most primitive one (E30) to perform the fractional crystallization modeling. The trachyte and fayalite-pyroxene syenite samples fall on the computed liquid line of descent. Almost all the hawaiites samples seem to be obtained by fractional crystallization of basanite E55.

The use of incompatible trace element ratios such as Rb/Nb, Nb/Y, Rb/Y, Th/La, Ce/Pb and La/Nb help us to monitor the influence of Pan-African basement assimilation on magma compositions. The low Rb/Nb (0.46–0.78) value of the Mbengwi recent felsic rocks and their positive slope on the Nb/Y vs. Rb/Y diagram (Fig. 14) clearly evidence the fact that they have not being contaminated by the basement. In addition, the range of Th/La (0.08–0.14), Ce/Pb (22.4–22.6) and La/Nb (0.83–0.66) ratios of the Mbengwi felsic lavas are similar to those of the uncontaminated less differentiated felsic lavas (LDFL) of the Bamenda mountains (Kamgang et al. 2010).

Petrogenesis of lavas and syenites

The similarity of isotopic signature of syenites and lavas, far from those of the Pan-African basement, and the parallel shape of their trace element patterns show that the investigated recent magmatic formations are genetically related, and belong to the same magmatic episode despite the observed compositional "Daly gap".

Several criteria can be emphasized in order to discuss the origin of the Mbengwi recent magmatic rocks. Although basaltic lavas are obviously originated from the mantle (occurrence of $Fo_{89–87}$ olivine and sometimes mantle xenocrysts), the relative low Ni content (179 ppm) of the least evolved lava shows that they erupted from an already differentiated mafic magma. The basalts derived from this magma through crystal

Table 5 Whole rock chemical analyses of representative samples from the Mbengwi recent magmatic formations. For the determinattion of εNd and εSr we use Chondritic uniform reservoir (CHUR) value after De Paolo and Wasserburg (1976) and Uniform reservoir (UR) after Vidal (1994)

	Basanites			Hawaiites					
Samples	E51	E30	E55	E4	E5	E7	E40	E43	E44
SiO_2	44.06	42.89	43.98	47.10	47.43	45.39	47.91	47.40	47.58
TiO_2	3.64	4.40	3.69	3.15	3.09	3.11	2.86	3.12	3.01
Al_2O_3	14.53	13.17	14.43	15.94	16.04	14.51	16.22	16.28	16.31
Fe_2O_3	1.80	1.80	1.79	1.73	1.74	1.54	1.73	1.76	1.73
FeO	12.02	12.03	11.91	11.52	11.59	10.29	11.56	11.73	11.54
MnO	0.21	0.19	0.19	0.21	0.21	0.18	0.22	0.22	0.23
MgO	7.25	11.17	7.46	4.96	4.70	8.39	4.24	4.65	4.72
CaO	10.54	10.26	10.13	7.75	8.16	9.76	8.02	8.17	8.06
Na_2O	3.10	2.12	3.41	4.37	3.99	4.18	4.20	3.79	3.89
K_2O	1.09	1.35	1.13	2.09	1.83	1.80	1.78	1.69	1.70
P_2O_5	1.76	0.60	1.90	1.18	1.22	0.84	1.27	1.19	1.23
TOTAL (wt.%)	100.00	100.00	100.00	100.00	100.00	100.00	100.00	100.00	100.00
DI	30.10	22.20	31.90	44.10	42.10	35.40	43.60	41.00	41.70
Na_2O+K_2O	4.19	3.47	4.53	6.46	5.82	5.98	5.98	5.48	5.59
Fe_2O_3/FeO	0.15	0.15	0.15	0.15	0.15	0.15	0.15	0.15	0.15
Norm CIPW									
Quartz	-	-	-	-	-	-	-	-	-
Orthoclae	6.44	7.99	6.65	12.38	10.82	10.66	10.53	10.00	10.06
Albite	20.56	9.87	21.10	25.45	28.36	12.26	30.28	29.65	30.15
Anorthite	22.50	22.45	20.78	17.70	20.47	15.49	20.15	22.41	22.02
Acmite	-	-	-	-	-	-	-	-	-
Sodium metasilicate	-	-	-	-	-	-	-	-	-
Leucite	-	-	-	-	-	-	-	-	-
Nepheline	3.09	4.35	4.18	6.23	2.91	12.52	2.83	1.32	1.48
Diopside	15.02	19.86	14.00	10.83	10.06	22.38	9.55	8.63	8.29
Larnite	-	-	-	-	-	-	-	-	-
Ortho Ca. Mg. Fe	0.00	0.00	0.00	0.00	0.00	0.00	0.00	0.00	0.00
Wollastonite	0.00	-	-	0.00	-	-	-	-	-
Hypersthene	-	-	-	-	-	-	-	-	-
Olivine	18.78	23.10	19.31	16.19	16.17	16.61	15.80	16.75	16.92
Magnetite	2.61	2.62	2.59	2.51	2.52	2.24	2.51	2.55	2.51
Ilmenite	6.91	8.36	7.00	5.99	5.87	5.91	5.43	5.93	5.71
Corundum	0.00	-	0.00	0.00	-	-	-	0.00	0.00
Apatite	4.08	1.39	4.40	2.74	2.83	1.94	2.93	2.76	2.86
TOTAL(wt.%)	100.00	100.00	100.00	100.00	100.00	100.00	100.00	100.00	100.00
Trace (ppm)									
Ag	0.09	0.07	0.09	0.19	0.20	0.11	0.23	0.22	0.23
Ba	390.56	538.72	338.97	464.17	476.31	572.57	486.84	478.15	489.96
Co	54.15	69.02	47.27	37.84	41.78	58.96	40.68	39.61	40.81
Cr	110.17	289.27	91.31	2.85	3.67	225.24	1.81	1.96	2.65
Cs	0.26	0.28	0.54	0.42	0.26	0.30	2.22	0.40	0.26

Table 5 (continued)

	Basanites			Hawaiites					
Samples	E51	E30	E55	E4	E5	E7	E40	E43	E44
Cu	36.19	32.94	29.46	21.23	21.91	39.30	15.75	19.39	19.06
Ga	21.26	18.18	20.17	25.71	27.44	21.47	27.46	26.81	27.46
Hf	3.38	2.92	3.19	7.12	7.23	3.99	7.7	7.3	7.29
Mo	1.42	1.39	1.22	3.48	2.92	3.55	2.90	3.15	2.96
Nb	46.01	41.25	45.33	101.68	104.01	73.26	107.29	104.26	106.17
Ni	65.91	179.35	53.08	15.22	11.86	124.28	7.03	11.89	9.85
Pb	2.22	1.61	1.90	3.71	3.78	2.66	3.86	3.67	3.79
Rb	20.32	20.72	21.53	55.45	32.09	36.78	40.87	28.76	33.59
Sn	1.63	1.46	1.74	2.74	2.71	2.81	3.29	2.79	3.21
Sr	1023.47	900.81	1028.45	790.74	985.90	863.44	1118.55	1130.10	1018.18
Ta	2.94	2.65	2.81	6.26	6.25	4.32	6.68	6.36	6.44
Th	3.26	2.75	3.11	7.51	7.81	5.63	8.08	7.75	8.11
Tl	0.04	0.09	b.d.	0.01	0.02	0.01	0.08	0.01	0.21
U	0.917	0.79	0.88	2.21	2.28	1.58	2.42	2.28	2.38
V	221.37	296.18	203.81	144.18	138.50	211.93	121.45	138.67	130.74
W	55.01	41.31	44.45	25.10	48.03	82.85	51.62	34.71	41.71
Zn	107.61	99.36	102.98	149.35	153.13	104.59	152.50	149.22	152.93
Zr	204.76	162.35	196.38	472.67	484.74	257.36	511.76	485.23	497.38
Y	29.76	21.42	29.79	33.90	34.92	24.94	35.09	34.37	34.59
La	45.71	27.31	45.67	74.28	77.24	46.75	80.13	76.86	79.29
Ce	102.97	59.85	103.26	154.75	160.84	91.79	165.77	159.58	164.09
Pr	13.61	7.81	13.54	18.20	18.85	10.67	19.33	18.80	19.11
Nd	59.41	34.28	59.91	71.24	73.25	43.42	75.30	73.13	74.18
Sm	11.46	7.25	11.92	12.97	13.21	8.37	13.42	13.08	13.26
Eu	4.01	2.51	4.06	3.77	3.89	2.77	4.00	3.95	3.97
Gd	10.81	7.10	10.92	11.10	11.29	8.13	11.54	11.49	11.77
Tb	1.33	0.90	1.32	1.42	1.45	1.02	1.45	1.46	1.44
Dy	7.03	4.96	6.78	7.73	7.97	5.62	7.88	7.72	7.76
Ho	1.17	0.83	1.16	1.32	1.32	0.99	1.37	1.34	1.35
Er	2.89	2.14	2.86	3.38	3.62	2.59	3.65	3.58	3.58
Tm	0.35	0.28	0.33	0.45	0.44	0.32	0.46	0.46	0.48
Yb	2.11	1.69	2.00	2.88	2.91	2.02	2.91	2.87	2.98
Lu	0.29	0.23	0.28	0.39	0.42	0.29	0.43	0.42	0.42
Isotopes									
$(^{87}Sr/^{86}Sr)_m$	0.703709	0.703574		0.703257					
2σ	0.000010	0.000010		0.000008					
$(^{143}Nd/^{144}Nd)_m$	0.512794	0.512855		0.512871					
2σ	0.000006	0.000006		0.000007					
$^{87}Rb/^{86}Sr$	0.055553	0.064333		0.196162					
$^{147}Sm/^{144}Nd$	0.125188	0.133718		0.111548					
$(^{87}Sr/^{86}Sr)_i$	0.703687	0.703548		0.703179					
$(^{143}Nd/^{144}Nd)_i$	0.512771	0.512830		0.512850					

Table 5 (continued)

	Basanites			Hawaiites					
Samples	E51	E30	E55	E4	E5	E7	E40	E43	E44
εNd	3.043083	4.233006		4.545118					
εSr	−12.645473	−14.561453		−19.060460					

	Hawaiites			mugearites	trachytes	rhyolites	Syenites		
Samples	E50	E7-1	E146	D15	E56	F3	F0	F1	BA83
SiO_2	47.39	45.83	47.37	49.86	62.63	76.00	64.81	63.80	63.44
TiO_2	3.09	2.92	3.09	2.42	0.78	0.50	0.57	0.57	0.62
Al_2O_3	16.01	14.58	16.20	16.19	16.97	10.37	15.34	16.70	16.71
Fe_2O_3	1.74	1.47	1.78	1.55	0.96	0.96	0.75	0.87	0.67
FeO	11.57	9.79	11.90	10.34	4.26	3.21	4.98	3.86	4.46
MnO	0.22	0.18	0.22	0.25	0.21	0.07	0.27	0.20	0.23
MgO	4.82	7.03	4.87	3.44	0.43	0.08	0.40	0.50	0.41
CaO	8.07	9.72	8.26	7.26	1.79	0.12	1.24	1.73	1.87
Na_2O	4.06	6.47	3.45	5.00	6.52	4.35	5.94	6.32	6.28
K_2O	1.84	1.17	1.70	1.98	5.20	4.29	5.56	5.28	5.18
P_2O_5	1.20	0.83	1.15	1.71	0.23	0.04	0.15	0.16	0.14
TOTAL (wt.%)	100.00	100.00	100.00	100.00	100.00	100.00	100.00	100.00	100.00
DI	42.30	42.70	39.30	51.70	86.00	89.70	84.70	86.20	84.80
Na_2O+K_2O	5.91	7.65	5.15	6.98	11.73	8.64	11.50	11.60	11.46
Fe_2O_3/FeO	0.15	0.15	0.15	0.15	0.225	0.30	0.15	0.225	0.15
Norm CIPW									
Quartz	-	-	-	-	-	34.84	3.85	1.47	1.02
Orthoclae	10.90	6.94	10.07	11.72	30.76	25.34	32.85	31.20	30.63
Albite	28.01	13.31	29.19	37.15	55.20	29.48	47.97	53.50	53.12
Anorthite	20.00	7.27	23.69	15.87	1.66	-	-	1.59	2.10
Acmite	-	-	-	-	-	2.79	2.01	-	-
Sodium metasilicate	-	-	-	-	-	0.97	-	-	-
Leucite	-	-	-	-	-	-	-	-	-
Nepheline	3.44	22.45	-	2.79	-	-	-	-	-
Diopside	10.16	29.06	8.15	7.55	4.98	0.30	4.53	5.13	5.44
Larnite	-	-	-	-	-	-	-	-	-
Ortho Ca. Mg. Fe	0.00	0.00	0.00	0.00	0.00	0.00	0.00	0.00	0.00

Table 5 (continued)

	Hawaiites			mugearites	trachytes	rhyolites	Syenites		
Samples	E50	E7-1	E146	D15	E56	F3	F0	F1	BA83
Wollastonite	-	-	-	-	-	-	-	-	-
Hypersthene	-	-	0.74	-	2.02	5.25	7.29	4.39	5.22
Olivine	16.33	11.37	17.04	14.11	1.99	-	-	-	-
Magnetite	2.52	2.13	2.59	2.25	1.39	0.00	0.08	1.26	0.97
Ilmenite	5.86	5.54	5.88	4.59	1.47	0.95	1.08	1.09	1.18
Corundum	-	-	-	0.00	-	-	-	-	-
Apatite	2.78	1.92	2.66	3.97	0.54	0.09	0.34	0.38	0.33
TOTAL(wt.%)	100.00	100.00	100.00	100.00	100.00	100.00	100.00	100.00	100.00
Trace (ppm)									
Ag	0.22	0.12	0.19	0.14	0.10	0.57	<1	<1	
Ba	483.85	552.04	475.37	692.21	2029.45	22.34	556.00	1365.00	25.30
Co	43.00	55.00	41.19	17.12	12.62	11.20	34.60	20.20	0.10
Cr	2.30	249.74	2.36	0.26	0.27	0.22	<10	<10	0.30
Cs	0.51	0.50	0.74	0.22	0.19	0.62	0.84	0.40	1.94
Cu	18.36	52.31	19.78	2.09	1.69	2.40	<5	<5	6.93
Ga	27.23	21.57	26.92	21.00	28.74	44.82	33.80	30.20	40.00
Hf	7.18	4.05	7.16	5.15	3.99	20.22	25.20	8.20	22.60
Mo	3.79	3.02	3.55	2.742	2.72	2.72	4.00	3.00	6.50
Nb	103.31	72.00	102.02	75.09	51.19	235.99	148.00	74.30	181.00
Ni	11.81	136.47	12.30	0.22	0.34	0.18	<5	<5	1.40
Pb	3.72	3.20	3.62	3.55	3.98	8.05	9.00	7.00	14.00
Rb	39.30	50.64	34.66	34.81	39.37	138.97	98.60	57.70	82.70
Sn	2.82	1.98476	2.96	1.71	1.69	8.10	7.00	2.00	5.93
Sr	1006.52	901.35	1065.98	1241.62	235.30	6.11	87.10	172.50	6.80
Ta	6.33	4.34	6.26	4.74	3.14	13.76	10.30	4.30	13.90
Th	7.90	6.15	7.75	5.48	3.63	22.20	17.10	5.70	17.10
Tl	0.03	b.d.	0.04	0.02	0.10	0.17	<0.5	<0.5	0.20
U	2.33	1.63	2.29	1.52	1.01	1.20	4.60	1.30	3.40
V	136.20	204.09	139.20	53.94	1.54	0.45	5.00	<5	0.20
W	58.10	62.10	46.03	22.53	57.73	55.04	171.00	99.00	0.93
Zn	149.68	104.37	147.10	120.24	110.13	142.95	170.00	129.00	460.00
Zr	481.74	265.82	477.66	330.67	239.82	1407.39	979.00	325.00	895.00
Y	35.13	25.08	34.24	33.31	24.66	95.40	70.10	33.30	97.90
La	76.48	46.76	76.28	64.58	42.89	155.95	86.60	60.30	187.90

Table 5 (continued)

	Hawaiites			mugearites	trachytes	rhyolites	Syenites		
Samples	E50	E7-1	E146	D15	E56	F3	F0	F1	BA83
Ce	158.81	90.75	157.79	139.35	89.65	180.83	181.00	122.00	355.40
Pr	18.76	10.62	18.58	17.24	10.90	39.16	20.30	13.80	42.30
Nd	73.48	41.90	72.56	70.31	43.51	144.80	80.00	54.60	160.90
Sm	13.33	8.32	13.00	12.97	8.24	28.31	15.75	10.05	29.20
Eu	3.88	2.68	3.83	4.58	5.22	1.96	3.35	4.44	4.70
Gd	11.28	7.75	11.21	11.73	7.36	23.89	15.25	9.35	23.30
Tb	1.45	1.02	1.41	1.42	0.98	3.62	2.53	1.40	3.30
Dy	7.83	5.49	7.52	7.55	5.47	21.04	13.45	7.20	18.90
Ho	1.35	0.99	1.31	1.32	0.94	3.63	2.69	1.35	3.70
Er	3.64	2.54	3.55	3.47	2.60	10.02	7.56	3.63	9.20
Tm	0.47	0.32	0.46	0.45	0.33	1.42	1.04	0.47	1.40
Yb	2.86	1.97	2.92	2.58	2.13	9.33	6.34	2.88	8.20
Lu	0.42	0.27	0.41	0.38	0.33	1.30	0.91	0.43	1.30
Isotopes									
$(^{87}Sr/^{86}Sr)_m$		0.703175	0.703403	0.704029	0.704025	0.727181	0.705545	0.704289	
2σ		0.000008	0.000008	0.000007	0.000008	0.000009	0.000006	0.000010	
$(^{143}Nd/^{144}Nd)_m$		0.512903	0.51287	0.512787	0.512708	0.512691	0.512702	0.512691	
2σ		0.000006	0.000004	0.000007	0.000007	0.000006	0.000006	0.000005	
$^{87}Rb/^{86}Sr$		0.157225	0.090951	0.078434	0.468331	63.777496	3.167472	0.935807	
$^{147}Sm/^{144}Nd$		0.123885	0.111788	0.11561	0.119513	0.122306	0.119068	0.111321	
$(^{87}Sr/^{86}Sr)_i$		0.703112	0.703367	0.703998	0.703838	0.701670	0.704278	0.703915	
$(^{143}Nd/^{144}Nd)_i$		0.512880	0.512849	0.512766	0.512686	0.512668	0.512680	0.512671	
εNd		5.169340	4.525611	2.906534	1.365486	1.033868	1.248444	1.033868	
εSr		−20.224241	−16.988362	−8.103889	−8.160658	320.479705	13.411865	−4.413852	

$_i$=initial $_m$=measured b.d.=below detection

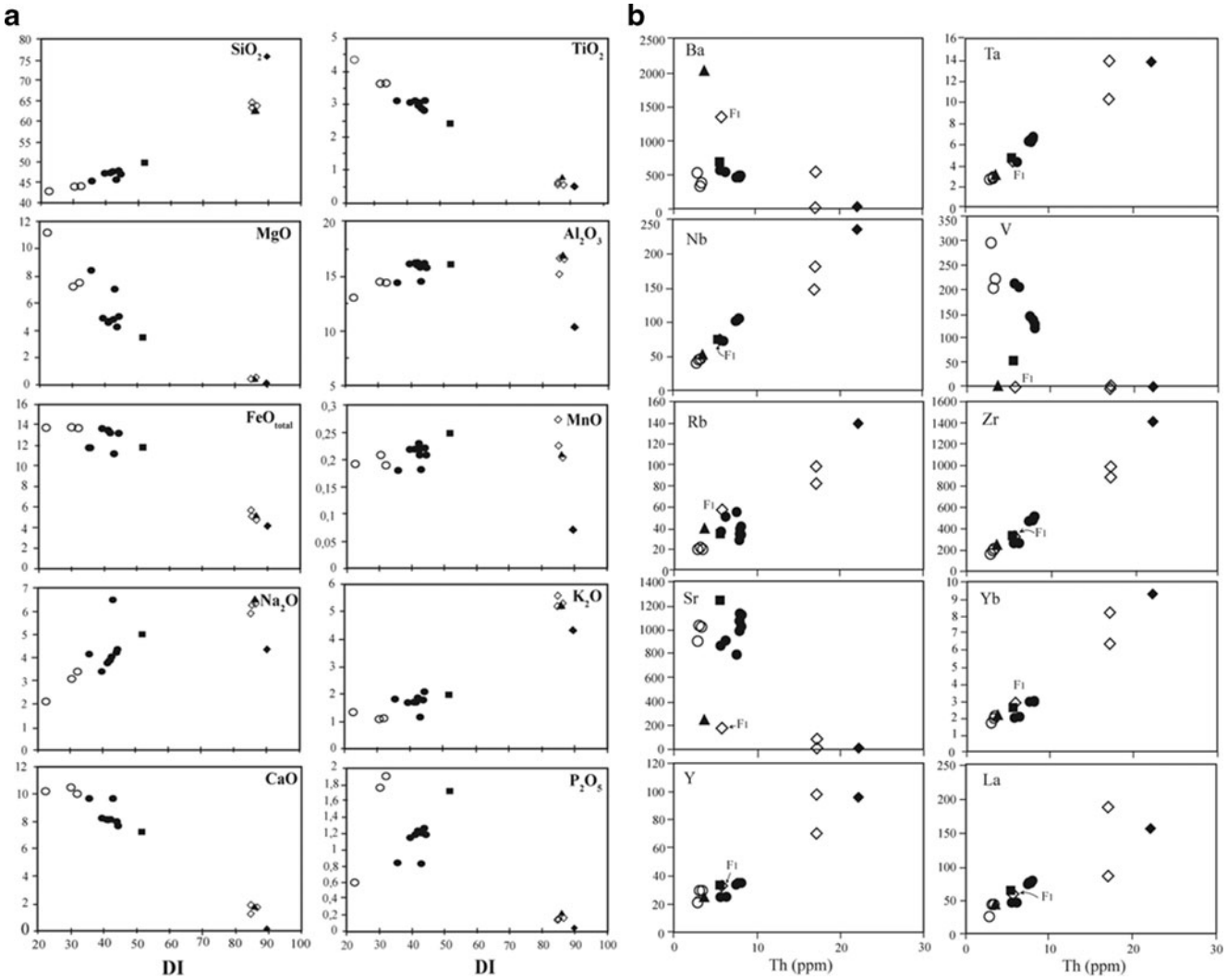

Fig. 8 (**a**) Major-element (wt. %) vs DI distribution of lavas. (**b**) Trace element distribution (Th vs. Ba, Nb, Rb, Sr, Y, Ta, V, Zr, Yb and La) for the Mbengwi recent magmatic rocks

fractionation of olivine, clinopyroxene, and Fe-Ti oxides, as it is the case for the whole CVL. The similarities of trace-element patterns and isotopic compositions observed between the Mbengwi basaltic lavas and the other basalts from the continental and oceanic sectors of the CVL (Fitton 1987, Ngounouno et al. 2000, 2003; Kamgang et al. 2008) and of Adamawa (Nono et al. 1994; Marzoli et al. 2000) are strong arguments in favor of a common mantle source. Basaltic lavas and trachytes from Mbengwi are probably related to the same mantle-derived magma source according to their similar Nb/Th and isotopic values.

The origin of peralkaline rhyolite magmas is still a long-standing debate as to know whether silicic magmas were formed by extended fractional crystallization of mafic parents (Macdonald et al. 2008) or by crustal anatexis. Given the generally phenocryst-poor nature of the rhyolites, extraction from the parental trachytic mushes must have been very efficient. The formation of these peralkaline rhyolites from metaluminous trachytes as described in the Bamenda Mountains may be possible after two stages of fractional crystallization accompanied by successive removal of respective quantities of alkali feldspar, amphibole, magnetite, olivine, clinopyroxene, and apatite (Kamgang et al. 2010). In fact, these peralkaline rhyolites should be seen as the final terms of successive fractional crystallization from basaltic lavas via trachytes.

Several genetic models have been proposed to interpret the formation of alkaline syenites, which mainly include: (1) fractional crystallization of amphibole, apatite, Fe–Ti oxides and later plagioclase from the parental

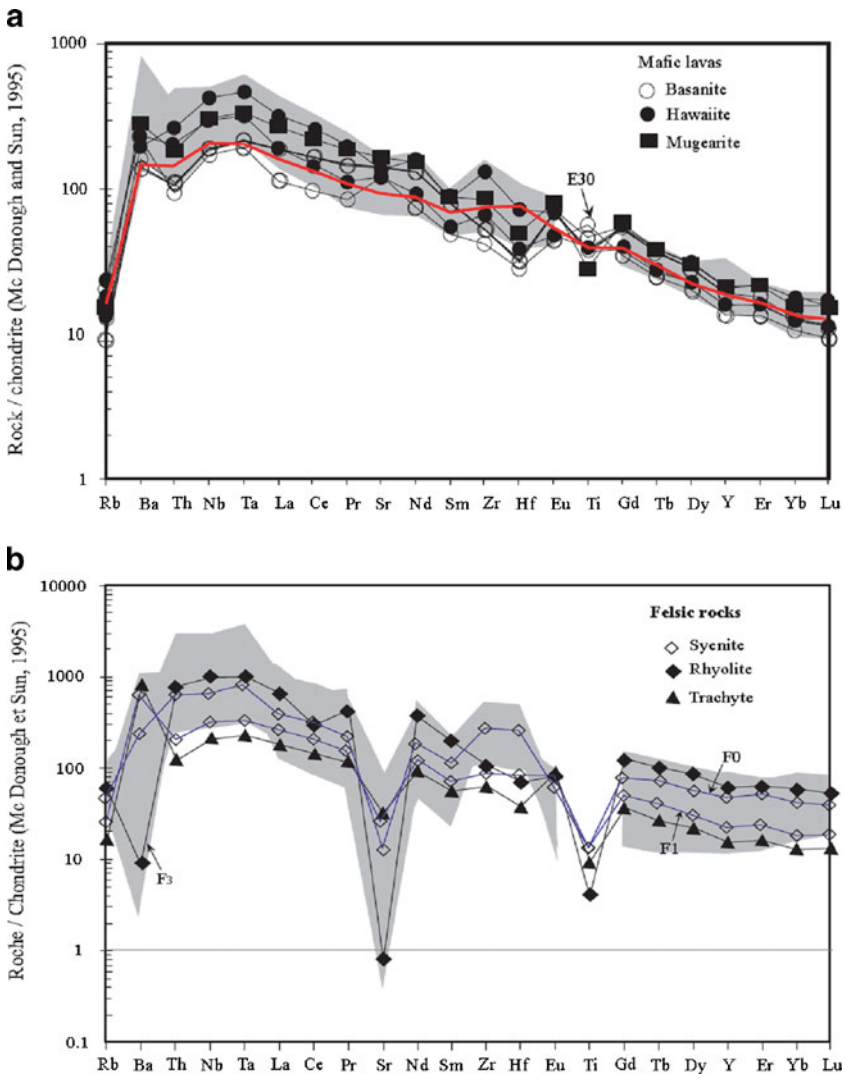

Fig. 9 Chondrite-normalized multi-element diagrams for mafic (**a**) and felsic rocks (**b**). The OIB pattern is in red color, data after Sun and McDonough (1989) Chondrite data after McDonough and Sun (1995). The grey field represents the composition of other similar rocks from CVL such as Bamenda (Kamgang et al. 2010), Mbépit (Wandji et al. 2008) Bambouto, Oku and Ngaoundere (Marzoli et al. 2000) for felsic rocks and Manengouba (Kagou Dongmo et al. 2001), Tombel grabben (Nkouathio et al. 2008), Mount Cameroon (Suh et al. 2003), Barombi Koto (Tamen et al. 2007), for mafic lavas

mantle-derived magmas (Litvinovsky et al. 2002) or fractional crystallization of precursor magmas, which were derived from enriched mantle sources once metasomatised by subducting sediments (Wang et al. 2005); (2) crustal assimilation and fractional crystallization (AFC) in mantle-derived basaltic magmas (Mingram et al. 2000) or (3) mixing of basaltic magma with crustal melt in variable proportions (Mingram et al. 2000; Vernikovsky et al. 2003). These two preceding processes produce hybrid magmas and the basic end-member must be strongly alkaline and enriched in incompatible trace elements. The hybrid melts are formed from an undepleted mantle source. The resulting syenites have metaluminous compositions, high potassium, high REE and LILE concentrations, with $^{87}Sr/^{86}Sr$ and ε_{Nd} ratios intermediate between crust and mantle.

As shown in Fig. 11 and confirmed by Fig. 13, syenites are in the trend of fractional crystallization. The Rb–Sr trend (Fig. 11) of the studied felsic rocks is not adequately reproduced by batch partial melting but by fractional crystallization from trachyte. The first hypothesis previously presented is the most likely for the Mbengwi syenites either metaluminous fayalite-pyroxene syenites or peralkaline quartz-syenites. As plutonic equivalent of trachytes, syenites were probably also formed by successive fractionation in depth from the same basaltic parental magma.

Nature and characteristics of sources

The mantle origin of the Mbengwi recent magmatic rocks is expressed both by low Sr isotopic ratios (0.7035–0.7053) and positive ε_{Nd} values. The position of all our syenites samples within the mantle A-type field in the ternary Nb–Ce–Y discrimination diagram (Eby, 1992) (not shown) also attests their mantle origin.

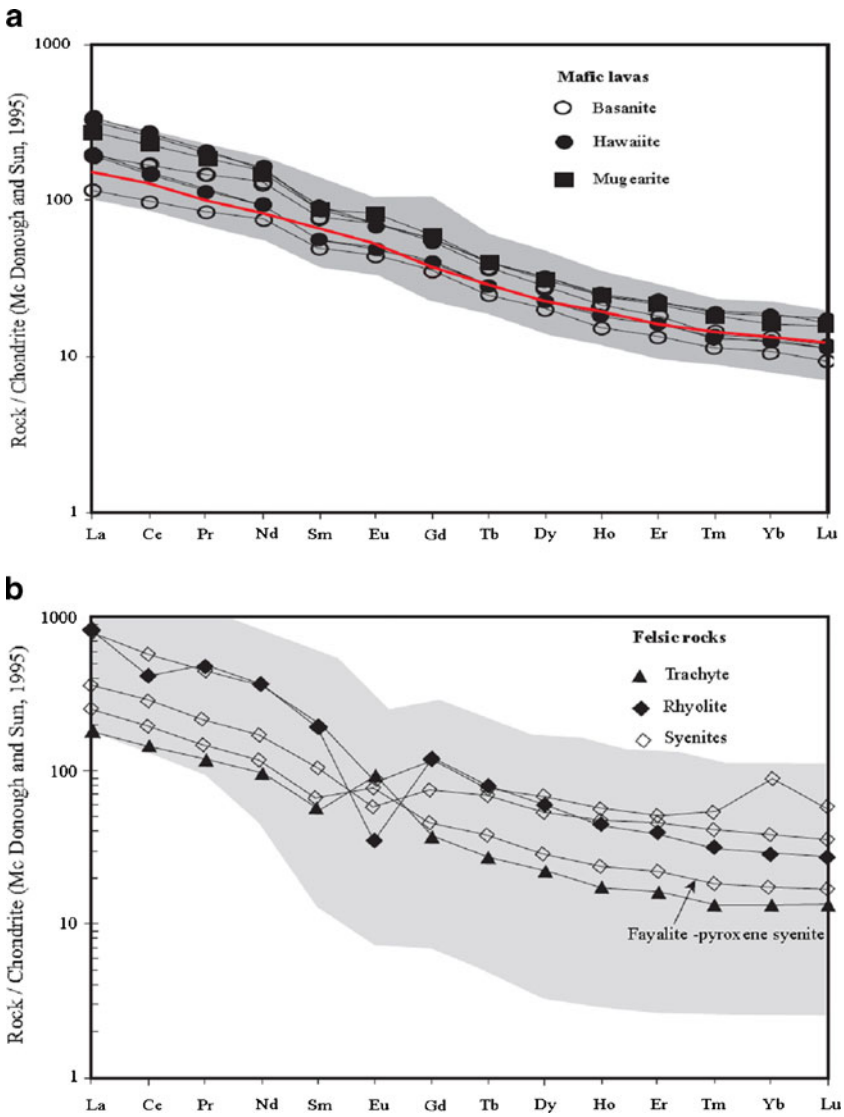

Fig. 10 Chondrite-normalized REE diagrams; the red pattern is for OIB according to the data after Sun and McDonough (1989), Chondrite data after McDonough and Sun (1995). The grey field represents the composition of other similar rocks from CVL such as Bamenda (Kamgang et al. 2010), Mbépit (Wandji et al. 2008) Bambouto, Fongo Tongo and Ngaoundere (Marzoli et al. 2000; Nkouandou et al. 2008) for felsic rocks and Bambouto, Adamaoua plateau (Marzoli et al. 1999), Manengouba (Kagou Dongmo et al. 2001), Tombel grabben (Nkouathio et al. 2008), Mount Cameroon (Suh et al. 2003) and Barombi Koto (Tamen et al. 2007) for mafic lavas

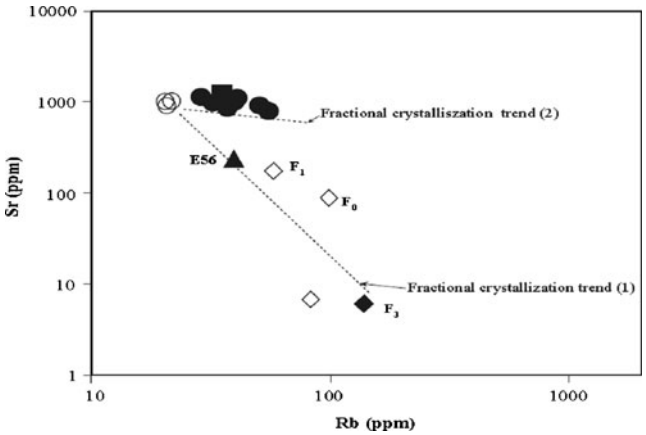

Fig. 11 Illustration of fractional crystallization in Rb vs. Sr diagram (Xu et al., 2007) for Mbengwi recent magmatic rocks showing that felsic rocks have evolved following twodifferent trends of fractionnal cristallization

The $\varepsilon_{Nd}>0$ and low initial $^{87}Sr/^{86}Sr$ of basaltic and trachytic rocks are similar to those of the other alkaline rocks from the CVL (0.7029–0.7039 after Déruelle et al. 2007) and suggest that they may result from a mixing between the original lower mantle primitive source and the depleted lithospheric mantle.

The values of the isotopic ratios of mafic and trachytic lavas very close to that of the chondritic uniform reservoir (CHUR=0.7046) probably mean that these rocks result from the melting of a very deep and enriched mantle material. The low $(Ce/Yb)_N$ values (9.3–14.9) for the Mbengwi magmas, when compared to those for other basalts of the CVL such as Mt Cameroon basalts $(Ce/Yb)_N \approx 15$, Benue Trough basalts $(Ce/Yb)_N \approx 19$ (Ngounouno et al. 2003), and the LREE enrichment may reflect low to medium degrees of mantle melting.

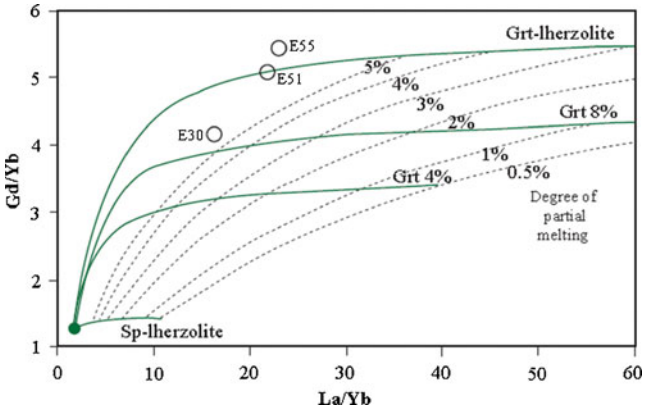

Fig. 12 Illustration of partial meling in Gd/Yb–La/Yb diagram. The Mbengwi lavas were plotted together with calculated curves for partial melting of a primitive mantle source (green filled circle in the lower left). Symbols are the same as other preceding figures. Two curves labeled Grt 4 % and 8 % represent the abundance of garnet in the source, corresponding to 20:80 and 40:60 proportions of Grt: Sp lherzolite. Accumulated fractional melting is assumed and partition coefficients reported in Halliday et al. (1995) are used in the calculation

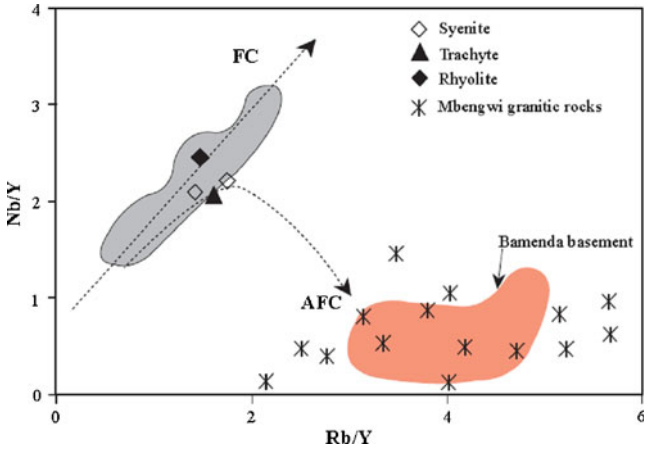

Fig. 14 Nb/Y versus Rb/Y after Cox and Hawkesworth (1985) and Leeman and Hawkesworth (1986) showing basement samples relative to the lava compositions. The grey field represents the composition of the Bamenda basaltic lavas. Data for Bamenda Precambrian basement are from Nzolang (2005)

Melting conditions of the Mbengwi recent magmatic rocks can be inferred from variations in the rare earth elements: LREE/HREE ratios are sensitive to the extent of melting, while MREE/HREE ratios are sensitive to the amount of residual garnet in the source. The range of $(Tb/Yb)_N$ ratios (2.05–2.93) in mafic lavas containing up to 6 wt.% MgO is higher than 1.7 and evidences the presence of garnet in the source as determined by Wang et al. 2002 for Basin and Range basalts. The Gd/Yb vs. La/Yb diagram (Fig. 12) reveals that, the Mbengwi data require more than 8 % of residual garnet in the source. Therefore, the variation of Gd/Yb ratios in the Mbengwi samples is due not only to fractional crystallization, but can also be explained by different degrees of melting (5–8 %) of a homogeneous source mantle.

Using the Nb/Y and Zr/Y ratios according to Condie (2005) (Fig. 15a), alkaline rocks of Mbengwi plot above the ΔNb line in the mantle plume field as defined by Fitton et al. (1997). It is suggested that these basalts have chemical features consistent with plume activity outlined by their OIB characters. The isotopic dataset illustrated by $^{87}Sr/^{86}Sr$ vs. $^{143}Nd/^{144}Nd$ diagram (Fig. 15b) suggest that the high $^{238}U/^{204}Pb$ (HIMU)

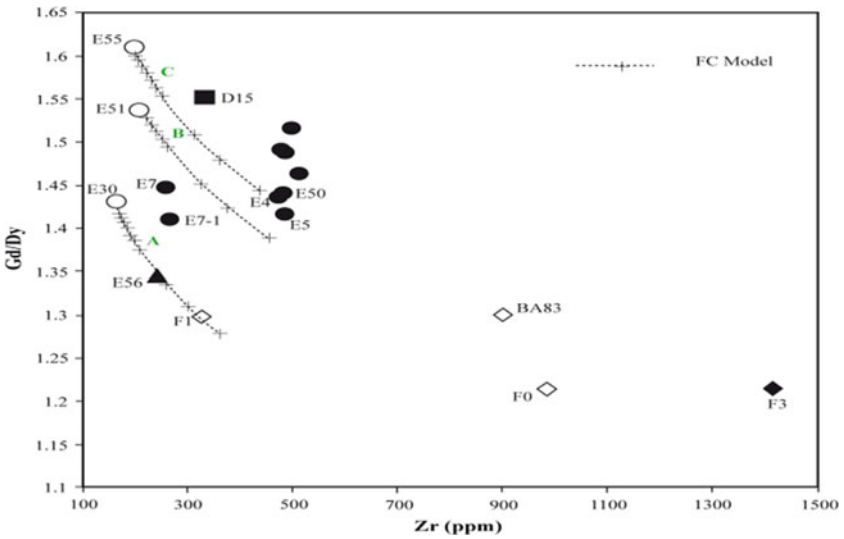

Fig. 13 Fractional crystallization modelling of the Mbengwi recent magmatic rocks using Gd/Y ration and. Zr contents. Several fractional crystallization trends were obtained. Trends labeled A correspond to fractional crystallization from the less evolved basanite (E30 to trachyte); trend labeled C correspond to fractional crystallization from basanite E55 to hawaiites

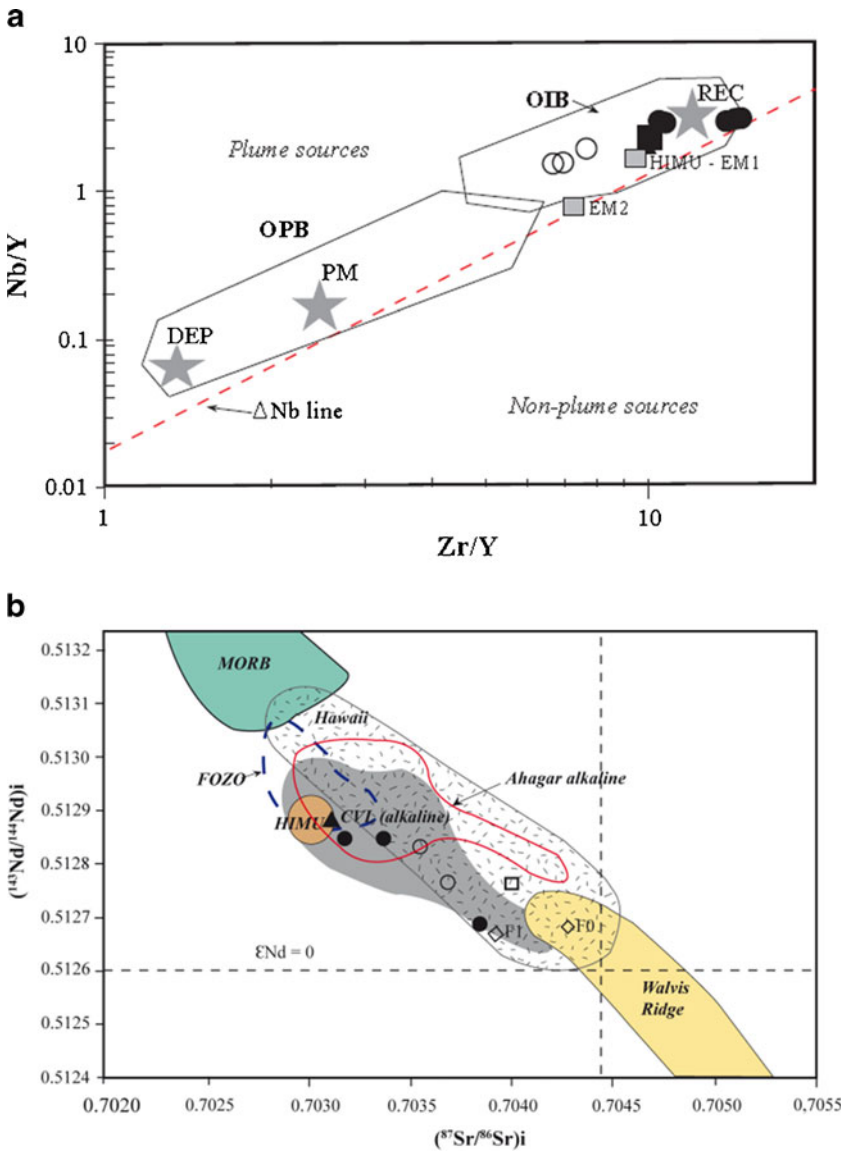

Fig. 15 (**a**) Plot of the Mbengwi recent magmatic rocks relative to the mantle compositional components (filled star) and fields for basalts from various tectonic settings as defined by Weaver (1991) and Condie (2005). DEP=deep depleted mantle; PM=primitive mantle; HIMU=high U/Pb mantle source; EM1=enriched mantle sources; REC=recycled component; PM=primitive mantle; DM=shallow depleted mantle; OIB=oceanic island basalt; OPB=oceanic plateau basalt. (**b**) Plot of the Mbengwi recent magmatic rocks in the isotopic $(^{87}Sr/^{86}Sr)_{initial}$ vs $(^{143}Nd/^{144}Nd)_{initial}$ diagram (adapted from Aït-Hamou et al. 2000; Moundi et al. 2007)

reservoir was involved in the genesis of the Mbengwi alkaline series. The trachyte, as all the late alkaline lavas is systematically located closer to the HIMU pole than the other samples, which suggests an increasing involvement with time of this pole in the genesis of the magmas. Hawaiites are largely influenced by recycled component (REC). The contribution of other components like enriched mantle (EM2) and focal zone (FOZO), if they exist would remain very weak. The similarities between the Mbengwi mafic lavas and OIB rare earth element and multi-elements patterns would really suggest the passage of a hotspot under the CVL lithosphere without however modifying its composition as evoked in some previous studies along the CVL (Halliday et al. 1990; Lee et al. 1994) but the lack of temporal migration of the magmatism precludes the existence of such a hotspot.

Conclusion

The Mbengwi recent magmatic rocks (≈ 28.2 Ma) are made up both of lavas and plutonites. Lavas form a bimodal alkaline series from basanite to rhyolites with a gap between 50 and 62 wt.%. Mafic rocks are essentially sodic while felsic rocks are sodic-potassic, slightly metaluminous to peralkaline. Trace elements are characterized by enrichment in HFSE and LREE compared with LILE and HREE respectively.

Basanites were generated by at least two different degrees of partial melting of the mantle. The main differentiation process is fractional crystallization with two different trends: the first includes basanite E30, trachyte and syenites, and the second basanite E55 and hawaiites. Basaltic and trachytic rocks have chemical features consistent with plume activity outlined by their OIB characters, and their isotopic ratios ($\varepsilon_{Nd}>0$ and low initial $^{87}Sr/^{86}Sr$). The Sr-Nd isotopic dataset suggest that the HIMU reservoir was involved in the genesis of the Mbengwi alkaline series.

These preliminary mineralogical and geochemical data for the Mbengwi recent magmatic formations provide important informations on magmatic events, petrogenetic processes and age of this area of the CVL. However, additional petrological and U-Pb geochemical studies are required for deep investigations and to further confirm preliminary conclusions.

Acknowledgements The French "Ministère des Affaires Etrangères" is acknowledged for providing grants to Benoît Joseph Mbassa for stays in France successively in the Laboratoire de Dynamisme Terrestre et Planétaire (DTP) then in the Laboratoire Géosciences-Environnement-Toulouse (GET), Université Paul Sabatier, Toulouse 3, and for financially supporting all the analysis. Fieldwork was substantially supported by the Institute of Geological and Mining research (IRGM) of Cameroon. Philippe De Parseval, Pierre Brunet all of the department Géosciences-Environnement-Toulouse (GET), France, A. Munilla of the University of Sevilla in Spain, and F. Gallice of the University of Saint Etienne, France are thanked for their technical help during data acquisition. The constructive reviews of two anonymous reviewers greatly improved the early version of this paper. For their help in discussing various aspects of this work during its preparation, we thank P. Moussango and Z. Itiga.

References

Aït-Hamou F, Dautria J-M, Cantagrel J-M, Dostal J, Briqueu L (2000) Nouvelles données géochronologiques et isotopiques sur le volcanisme cénozoïque de l'Ahaggar (Sahara algérien): des arguments en faveur de l'existence d'un panache. C R Acad Sci Paris, Ser IIa 330(12):829–836

Aries S, Valladon M, Polvé M, Dupré B (2000) A routine method for oxide and hydroxide interference corrections in ICP-MS chemical analyses of environmental and geological samples. Geostandards Newsletter 24:19–31

Benoit M, Polvé M, Ceuleneer G (1996) Trace element and isotopic characterization of mafic cumulates in a fossil mantle diapir (Oman ophiolite). Chem Geol 134:199–214

Burke K (2001) Origin of the Cameroon Line of volcano-capped swells. J Geol 109:349–362

Condie KC (2005) High field strength element ratios in Archean basalts: a window to evolving sources of mantle plume. Lithos 79:491–504

Cox KG, Hawkesworth C (1985) Geochemical stratigraphy of the Deccan traps at Mahabaleshwar, western Ghats, India, with implications for open system magmatic processes. J Petrol 26:355–377

Davidson PM (1994) Ternary iron, magnesium, calcium carbonates: A thermodynamic model for dolomite as an ordered derivative of calcite-structure solutions. Am Mineral 79:332–339

Deer WA, Howie RA, Zussman J (1992) An introduction to the rock forming minerals. Prentice Hall, NY, p 712

De Paolo DI, Wasserburg GJ (1976) Nd isotopic variations and petrogenetic models. Geophys Res Lett 3:249–253

Déruelle B, Ngounouno I, Demaiffe D (2007) The "Cameroon hot line" (CHL): A unique example of active alkaline intraplate structure in both oceanic and continental lithospheres. CR Geosci 339:589–600

Duchesne JC, Demaiffe D (1978) Trace elements and anorthosite genesis. Earth Planet Sci Lett 38:249–272

Eby GN (1992) Chemical subdivision of A-type granitoids: Petrogenetic and tectonic implications. Geol 20:641–644

Fitton J G (1987) The Cameroon Line, West Africa: a comparison between oceanic and continental volcanism. In: Fitton J G, Upton B G J. (Eds.), Alkaline Igneous Rocks. Geol. Soc. London Spec. Pub. 30: 273–291

Fitton JG, Saunders AD, Norry MJ, Hardarson BS, Taylor RN (1997) Thermal and chemical structure of the Iceland plume. Earth Planet Sci Lett 153:197–208

Giret A (1983) Le plutonisme océanique intraplaque: Exemple des iles Kerguelen. Mémoire CNFRA 54:290

Gountié Dedzo M, Nédélec A, Nono A, Njanko TE, Font E, Kamgang P, Njonfang E, Launeau P (2011) Magnetic fabrics of the Miocene ignimbrites from West-Cameroon: Implications for pyroclastic flow source and sedimentation. J Vol Geoth Res 203:113–132

Haggerty S E, Tompkins L A (1983) Subsolidus reactions in Kimberlitic ilmenites: Exsolution, reduction and the redox state of the mantle. Proc. 3rd Int. Kimb. Conf.

Halliday AN, Davidson JP, Holden P, DeWolf C, Lee D-C, Fitton JG (1990) Trace element fractionation in plumes and the origin of HIMU mantle beneath the Cameroon line. Nature 347:523–528

Halliday AN, Lee D-C, Tommasini S, Davies GR, Paslick CG, Fitton JG, James DE (1995) Incompatible trace elements in OIB and MORB and source enrichment in the sub-oceanic mantle. Earth Planet Sci Lett 133:379–395

Hanson G (1980) Rare earth elements in petrogenetic studies of igneous systems. Annual Review Earth Planet. Sci., 371–406.

Kagou Dongmo A, Wandji P, Pouclet A, Vicat JP, Cheilletz A, Nkouathio DG, Alexandrov P, Tchoua FM (2001) Évolution volcanologique du mont Manengouba (Ligne du Cameroun); nouvelles données pétrographiques, géochimiques et géochronologiques. C R Acad Sci 333:155–162

Kagou Dongmo A, Nkouathio DG, Pouclet A, Bardintzeff J-M, Wandji P, Nono A, Guillou H (2010) The discovery of late Quaternary basalt on Mount Bambouto: Implications for recent widespread volcanic activity in the southern Cameroon Line. J Afr Earth Sci 57:96–108

Kamenetsky VM, Crawford AJ, Meffre S (2001) Factors controlling chemistry of magmatic spinel: an Empirical study of associated olivine, Cr-spinel and Melt Inclusions from primitive rocks. J Petrol 42(4):655–671

Kamgang P, Njonfang E, Chazot G, Tchoua F (2007) Géochimie et géochronologie des laves felsiques des monts Bamenda (ligne volcanique du Cameroun). CR Geosci 339(10):659–666

Kamgang P, Chazot G, Njonfang E, Tchoua FM (2008) Geochemistry and geochronology of mafic rocks from Bamenda Mountains (Cameroon): Source composition and crustal contamination along the Cameroon Volcanic Line. CR Geosci 340:850–857

Kamgang P, Njonfang E, Nono A, Gountie Dedzo M, Tchoua FM (2010) Petrogenesis of a silicic magma system: Geochemical evidence from Bamenda Mountains, NW Cameroon. Cameroon Volcanic Line J Afr Earth Sci 58:285–304

Leake BE et al (1997) Nomenclature of amphiboles: report of the subcommittee on amphiboles of the International Mineralogical Association, commission on new minerals and mineral names. Am Mineral 82:1019–1037

Le Bas MJ, Le Maître RW, Streckeisen A, Zanettin B (1986) A chemical classification of volcanic rocks based on the total alkali-silica diagram. J Petrol 27:745–750

Lee D-C, Halliday AN, Fitton JG, Poli G (1994) Isotopic variations with distance and time in the volcanic islands of the Cameroon line: Evidence for a mantle plume origin. Earth Planet Sci Lett 123:119–138

Leeman WP, Hawkesworth C (1986) Open magma systems: trace element and isotopic constraints. J Geophys Res 91(B6):5901–5912

Litvinovsky AA, Jahn BM, Zanvilevich AN, Saunders A, Poulain S, Kuzmin DV, Reichow MK, Titov AV (2002) Petrogenesis of syenite–granite suites from the Bryansky Complex (Transbaikalia, Russia): implications for the origin of A-type granitoids magmas. Chem Geol 189:105–133

Macdonald R, Katsura T (1964) Chemical composition of Hawaiian lavas. J Petrol 5(1):82–133

Macdonald R, Belkin HE, Fitton JG, Rogers NW, Nejbert K, Tindle AG, Marshall AS (2008) The roles of fractional crystallization, magma mixing, crystal mush remobilization and volatile melt interactions in the genesis of a young basalt peralkaline rhyolite suite, the greater OlkariaVolcanic complex, Kenya rift valley. J Petrol 49(8):1515–1547

Marzoli A, Renne PR, Peccirillo EM, Castorina F, Bellieni G, Melfi AG, Nyobe JB, N'ni J (1999) Silicic magmas from the continental Cameroon Volcanic Line (Oku, Bambouto and Ngaoundere): ^{40}Ar–^{39}Ar dates, petrology, Sr–Nd–O isotopes and their petrogenetic significance. Contrib Mineral Petrol 135:133–150

Marzoli A, Piccirillo EM, Renne PR, Bellieni G, Iacumin M, Nyobe JB, Tongwa AT (2000) The Cameroon Volcanic Line revisited: Petrogenesis of continental basaltic magmas from lithospheric and asthenospheric mantle sources. J Petrol 41:87–109

McDonough WF, Sun SS (1995) The composition of the Earth. Chem Geol 120:223–253

Mingram B, Trumbull RB, Littman S, Grettenberger H (2000) A petrogenetic study of androgenic felsic magmatism in the Cretaceous Paresis ring complex, Namibia: evidence for mixing of crust and mantle-derived components. Lithos 54:1–22

Morimoto N, Fabriès J, Ferguson AK, Ginzburg IV, Ross M, Seifert FA, Zussman J, Aoki K, Gottardi G (1988) Nomenclature of pyroxenes. Am Mineral 73:1123–1133

Moundi A, Wandji P, Bardintzeff J-M, Ménard J-J, Okomo Atouba LC, Mouncherou OF, Reusser E, Bellon H, Tchoua FM (2007) Les basaltes éocènes à affinité transitionnelle du plateau Bamoun, témoins d'un réservoir mantellique enrichi sous la ligne volcanique du Cameroun. CR Geosci 339:396–406

Ngounouno I, Déruelle B, Demaiffe D (2000) Petrology of the bimodal Cenozoic volcanism of the Kapsiki plateau (northernmost Cameroon, Central Africa). J Volcanol Geoth Res 102:21–44

Ngounouno I, Déruelle B, Bardintzeff JM (2001) Wehrlite and clinopyroxenite xenoliths from Mt Cameroon: implications for lithospheric processes. XI European union of geosciences meeting, Strasbourg, 8–12 April 2001. J Conf Abstr 6(1):474–475

Ngounouno I, Déruelle B, Demaiffe D, Montigny R (2003) Petrology of Cenozoic volcanism in the Upper Benue valley, northern Cameroon (Central Africa). Contrib Mineral Petrol 145:87–106

Njonfang E, Moreau C (1996) The mineralogy and geochemistry of a subvolcanic alkaline complex from the Cameroon Line: the Nda Ali massif, southwest Cameroon. J Afr Earth Sci 22 (2):113–132

Nkouandou FO, Ngounouno I, Déruelle B, Ohnenstetter D, Montigny R, Demaiffe D (2008) Petrology of the Mio-Pliocene volcanism to North and East of Ngaoundéré (Adamawa, Cameroon). CR Geosci 340:28–37

Nkouathio D G (1997) Le volcanisme récent du graben de Tombel (provinces du Littoral et du Sud-ouest, Cameroun): volcanologie, géochimie, pétrologie et valeurs agricoles. Thèse Doct. 3^{e} cycle, 179p. Univ. Yaoundé I, Cameroun.

Nkouathio DG, Kagou Dongmo A, Bardinzeff JM, Wandji P, Bellon H, Pouclet A (2008) Evolution of volcanism in graben and horst structures along the Cenozoic Cameroon Line (Africa): implications for tectonic evolution and mantle source composition. Contrib Mineral Petrol 94:287–303

Nono A, Déruelle B, Demaiffe D, Kambou R (1994) Tchabal Nganha volcano in Adamawa (Cameroon): petrology of a continental alkaline lava series. J Vol Geo Res 60:147–178

Nonnotte P, Benoit M, Le Gall B, Hémond C, Rolet J, Cotten J, Brunet P, Makoba E (2011) Petrology and geochemistry of alkaline lava series, Kilimanjaro, Tanzania: New constraints on petrogenetic processes, *in* Beccaluva L, Bianchini G, and Wilson M, eds., Volcanism and Evolution of the African Lithosphere. Geol. Soc. Am. Spec. Paper 478:1–32.4

Nzolang C (2005) Crustal evolution of the Precambrian basement in west Cameroon: inference from geochemistry, Sr–Nd isotopic and experimental investigation of some granitoids and metamorphic rocks. PhD Thesis, Graduate School of Science and Education. Niigata University, Japan, p 207

Nzolang C, Kagami H, Nzenti JP, Holtz F (2003) Geochemistry and preliminary Sr–Nd isotopic data on the Neoproterozoic granitoids from the Bantoum area, west Cameroon. Evidence for a derivation from a Paleoproterozoic to Archean crust. Polar Geosci 16:196–226

Ore Research and Exploration (2004) Certificate of analysis for ferruginous soil secondary reference material OREAS 45P Report 04/512_rev2, 37p.

Smith JV, Brown WL (1988) Feldspar Minerals: Second Revised and Extended Edition. Springer Verlag, Berlin Heidelberg

Suh CE, Sparks RSJ, Fitton JG, Ayonghe SN, Annen C, Nana R, Luckman A (2003) The 1999 and 2000 eruptions of Mount Cameroon: eruption behaviour and petrochemistry of lava. Bull Volcanol 65:267–281

Sun S-S, McDonough WF (1989) Chemical and isotopic systematics of oceanic basalts: implications for mantle composition and processes. In: A D. Saunders and MJ. Norry (Eds). Magmatism in the Ocean Basins. Geol. Soc. London. 313–345.

Tamen J, Nkoumbou C, Mouafo L, Reusser E, Tchoua F (2007) Petrology and geochemistry of monogenetic volcanoes of the Barombi Koto volcanic field (Kumba graben, Cameroon). C R Geosci 339:799–809

Taylor SR, McLennan SM (1985) The continental crust: Its composition and evolution. Blackwell Scientific Pub, Oxford, 312p

Toteu SF, Van Schmus RW, Penaye J, Michard A (2001) New U–Pb and Sm–Nd data from north-central Cameroon and its bearing on the pre-Pan-African history of central Africa. Precamb Res 108:45–73

Vernikovsky VA, Pease VL, Vernikovskaya AE, Romanov AP, Gee DG, Travin AV (2003) First report of early Triassic A-type granite and syenite intrusions from Taimyr: Product of the northern Eurasian superplume. Lithos 66:23–66

Vidal P (1994) Géochimie. Dunod, Paris, p 190

Wang K, Plank T, Walker J D, Smith E I (2002) A mantle melting profile across the Basin and Range, SW USA. J. Geoph. Res. 107 (B1).

Wang Q, Li J-W, Jian P, Zhao Z-H, Xiong X-L, Bao Z-W, Xu J-F, Li C-F, Ma J-L (2005) Alkaline syenites in eastern Cathaysia (South China): link to Permian–Triassic transtension Earth. Planet Sci Lett 230:339–354

Wandji P (1995) Le volcanisme récent de la plaine du Noun (Ouest-Cameroun). Volcanologie, pétrologie, géochimie et pouzzolanicité. Thèse Doct. Etat, Univ. Yaoundé I, Cameroun, 295p.

Wandji P, Bardintzeff J-M, Ménard J-J, Tchoua F-M (2000) The alkaline fassaite bearing volcanic province of Noun plain (West-Cameroon). N Jahrb Miner Mh 1:1–14

Wandji P, Tchokona S, Bardintzeff J-M, Bellon H, Platevoet B (2008) Rhyolites of the Mbèpit Massif in the Cameroon volcanic line: an

early extrusive volcanic episode of Eocene age. Mineral Petrol 94:271–286

Wandji P, Tsafack JPF, Bardintzeff JM, Nkouathio DG, Kagou DA, Bellon H, Guillou H (2009) Xenoliths of dunites, wehrlites and clinopyroxenites in the basanites from Batoke volcanic cone (Mount Cameroon, Central Africa): petrogenetic implications. Mineral Petrol 96:81–98

Wass SY (1979) Multiple origins of clinopyropxenes in basaltic rocks. Lithos 12:115–132

Weaver BL (1991) The origin of ocean island basalt end-member compositions: trace element and isotopic constraints. Earth Planet Sci Lett 104:381–397

Weis D, Frey FA (1991) Isotope geochemistry of the Ninetyeast Ridge basement basalts: Sr, Nd, and Pb evidence for involvement of the Kerguelen hot spot. Proc Ocean Drill Program Sci Results 121:591–610

Xu C, Huang Z, Qi L, Fu P, Liu C, Li E, Gung T (2007) Geochemistry of Cretaceous granites from Mianning in the Panix region, Sichuan Province, southwestern China: implications for their generation. J Asi Earth Sci 29:737–750

Yokoyama T, Aka FT, Kusakabe M, Nakamura E (2007) Plume–lithosphere interaction beneath Mt. Cameroon volcano, West Africa: Constraints from 238U–230Th–226Ra and Sr–Nd–Pb isotope systematic. Geochim Cosmochim Acta 71:1835–1854